

DOI: 10.1002/chem.201202596

Synthesis and Self-Organization of Zinc  $\beta$ -(Dialkoxyphosphoryl)porphyrins in the Solid State and in SolutionEkaterina V. Vinogradova,<sup>[a]</sup> Yulia Y. Enakieva,<sup>[a, b]</sup> Sergey E. Nefedov,<sup>[b]</sup>  
Kirill P. Birin,<sup>[a, b]</sup> Aslan Y. Tsivadze,<sup>[a, b]</sup> Yulia G. Gorbunova,<sup>\*,[a, b]</sup>  
Alla G. Bessmertnykh Lemeune,<sup>[c]</sup> Christine Stern,<sup>[c]</sup> and Roger Guilard<sup>\*,[c]</sup>

**Abstract:** The first synthesis and self-organization of zinc  $\beta$ -phosphorylporphyrins in the solid state and in solution are reported.  $\beta$ -Dialkoxyphosphoryl-5,10,15,20-tetraphenylporphyrins and their Zn<sup>II</sup> complexes have been synthesized in good yields by using Pd- and Cu-mediated carbon-phosphorous bond-forming reactions. The Cu-mediated reaction allowed to prepare the mono- $\beta$ -(dialkoxyphosphoryl)porphyrins **1Zn–3Zn** starting from the  $\beta$ -bromo-substituted zinc porphyrinate ZnTPPBr (TPP = tetraphenylporphyrin) and dialkyl phosphites HP(O)(OR)<sub>2</sub> (R = Et, *i*Pr, *n*Bu). The derivatives **1Zn–3Zn** were obtained in good yields by using one to three equivalents of CuI. When the reaction

was carried out in the presence of catalytic amounts of palladium complexes in toluene, the desired zinc derivative **1Zn** was obtained in up to 72% yield. The use of a Pd-catalyzed C–P bond-forming reaction was further extended to the synthesis of  $\beta$ -poly(dialkoxyphosphoryl)porphyrins. An unprecedented one-pot sequence involving consecutive reduction and phosphorylation of H<sub>2</sub>TPPBr<sub>4</sub> led to the formation of a mixture of the 2,12- and 2,13-bis(dialkoxy)phosphorylporphyrins **5H<sub>2</sub>** and **6H<sub>2</sub>** in 81% total yield. According

to the X-ray diffraction studies, **1Zn** and **3Zn** are partially overlapped cofacial dimers formed through the coordination of two Zn centers by two phosphoryl groups belonging to the adjacent molecules. The equilibrium between the monomeric and the dimeric species exists in solutions of **1Zn** and **3Zn** in weakly polar solvents according to spectroscopic data (UV/Vis absorption and NMR spectroscopy). The ratio of each form is dependent on the concentration, temperature, and traces of water or methanol. These features demonstrated that zinc  $\beta$ -phosphorylporphyrins can be regarded as new model compounds for the weakly coupled chlorophyll pair in the photosynthesis process.

**Keywords:** aggregation • phosphonates • porphyrins • self-organization • transition metals

## Introduction

Porphyrin synthesis has attracted a large number of researchers in chemistry, physics, material science, engineering, biology, and medicine.<sup>[1]</sup> Indeed, structural, photophysical, magnetic, electrical, and catalytic properties of these tetrapyrrolic macrocycles are widely observed in natural and artificial processes. Their optical properties, for example, make them attractive for various photonic applications such as photodynamic therapy (PDT) of tumors,<sup>[2–4]</sup> holographic data storage,<sup>[5,6]</sup> optical power limiting,<sup>[7–11]</sup> and sensing.<sup>[12–15]</sup> Moreover, various porphyrin architectures assembled through non-covalent bonds find further applications in many fields, such as, for example, they are used to mimic the photosynthetic mechanism, to design efficient light-harvesting systems, or to prepare porous materials for gas molecules storage.<sup>[16–19]</sup> Thus, much effort has been devoted to the synthesis of new classes of metalloporphyrins bearing peripheral donor groups at the  $\beta$ -pyrrolic and/or the *meso*-positions of the porphyrin core to elaborate coordination networks and polynuclear species.<sup>[20]</sup> Recently, phosphorousubstituted porphyrins have arisen as promising molecular blocks for the design of coordination networks. Indeed, polynuclear systems and 1D coordination polymers have been

- [a] E. V. Vinogradova, Dr. Y. Y. Enakieva, Dr. K. P. Birin, Prof. A. Y. Tsivadze, Prof. Y. G. Gorbunova  
Russian Academy of Sciences  
Frumkin Institute of Physical Chemistry and Electrochemistry  
Leninsky pr., 31, GSP-1, 119071, Moscow (Russia)  
Fax: (+7) 495 952-25-66  
E-mail: yulia@igic.ras.ru
- [b] Dr. Y. Y. Enakieva, Prof. S. E. Nefedov, Dr. K. P. Birin, Prof. A. Y. Tsivadze, Prof. Y. G. Gorbunova  
Russian Academy of Sciences  
Kurnakov Institute of General and Inorganic Chemistry  
Leninsky pr., 31, GSP-1, 119991, Moscow (Russia)  
Fax: (+7) 495 952-25-66  
E-mail: yulia@igic.ras.ru
- [c] Dr. A. G. Bessmertnykh Lemeune, Dr. C. Stern, Prof. R. Guilard  
Institut de Chimie Moléculaire de l'Université de Bourgogne  
(ICMUB-UMR CNRS 6302)  
9 Avenue Alain Savary-BP 47870  
21078 Dijon Cedex (France)  
E-mail: Roger.Guilard@u-bourgogne.fr

Supporting information for this article is available on the WWW under <http://dx.doi.org/10.1002/chem.201202596>.

synthesized from mono-substituted *meso*-phosphoryl metalloporphyrins (M=Zn, Mg, Ni, Pd).<sup>[21–25]</sup> *Meso*-5,15-di(diethoxyphosphoryl)porphyrinatozinc building blocks have also been successfully used to prepare a 2D coordination network.<sup>[26]</sup> Self-organization of this metalloporphyrin proceeds more easily than the assembling of *meso*-5,15-di(4-diethoxyphosphoryl)porphyrinatozinc molecules, because direct attachment of the electron-withdrawing diethoxyphosphoryl substituent at the *meso*-position of the tetrapyrrolic macrocycle increases the affinity of the metal cation to the axial ligand.<sup>[27]</sup> The  $\beta$ -substituted derivatives commonly used to form porphyrin supramolecular systems in Nature demonstrate the potential utility of  $\beta$ -diethoxyphosphoryl-substituted porphyrins as precursors of self-assembling systems. To the best of our knowledge, the synthesis of these porphyrin derivatives has not been described so far.

A few decades ago, porphyrins were mainly prepared from pyrroles, which are readily obtained from acyclic precursors. Modification of a preformed porphyrin backbone was used predominantly for natural (e.g., protoporphyrin, hematoporphyrin), low-cost porphyrins, however this approach was limited to a basic substitution pattern. Recently, transition-metal-catalyzed reactions have been used to develop a new powerful synthetic strategy for the post-modification of porphyrin macrocycles. Indeed, transition-metal-mediated carbon–carbon and carbon–heteroatom (N, O, S, Se, P, B) bond forming reactions allow an efficient synthesis of a large number of porphyrin derivatives starting from halogenated precursors.<sup>[28–38]</sup> The versatility of this methodology has been demonstrated in many applications, including the synthesis of natural products, pharmaceuticals, and other key biologically active compounds, new ligands, and advanced materials. Generally, readily accessible *meso*-haloporphyrins were used as precursors. The reactivity of  $\beta$ -bromoporphyrins has been studied less, although Pd-catalyzed carbon–carbon bond-forming reactions have been first described over twenty-five years ago.<sup>[39–46]</sup>

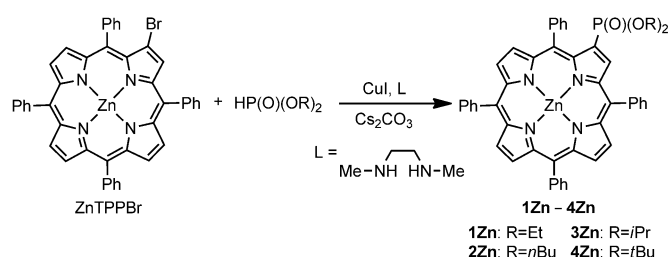
The studies related to the  $\beta$ -functionalization of porphyrins are often limited by the availability of the starting  $\beta$ -haloporphyrins. Regioselective substitution reactions with iodine and chlorine atoms have been described,<sup>[40,47–50]</sup> however  $\beta$ -bromoporphyrins still remain the most easily accessible  $\beta$ -halogenated derivatives.<sup>[51,52]</sup> A number of different procedures have been described for the synthesis of  $\beta$ -octabromo-substituted porphyrins.<sup>[53–58]</sup> Regioselective bromination at selected  $\beta$ -positions represents a more challenging task, however, recent improvements of synthetic procedures for 2-mono-,<sup>[59,60]</sup> 2,3-di-,<sup>[59,61,62]</sup> 2,3,12,13-tetra-,<sup>[63]</sup> and 2,3,7,8,12,13-hexabromoporphyrins<sup>[61]</sup> made these derivatives more accessible for further preparation of a large variety of functionalized porphyrins. For example, 2-bromo-5,10,15,20-tetraphenylporphyrin (H<sub>2</sub>TPPBr) was transformed into a variety of  $\beta$ -functionalized porphyrins through Pd-catalyzed carbon–heteroatom (N, O, S) bond-forming reactions.<sup>[60]</sup>

Herein, we extend the scope of transition-metal-mediated carbon–phosphorous bond-forming reactions to  $\beta$ -bromoporphyrins. The self-organization of the new class of  $\beta$ -phos-

phorylporphyrins in the solid state and in solution is also studied. The described results clearly demonstrate that  $\beta$ -phosphoryl-substituted metalloporphyrins is prospective building blocks to elaborate supramolecular ensembles and coordination networks.

## Results and Discussion

**Synthesis of  $\beta$ -(dialkoxyphosphoryl)porphyrins:** H<sub>2</sub>TPPBr was chosen as the starting halide precursor, because this compound is readily available by a standard bromination procedure.<sup>[60,64]</sup> First, the reaction of H<sub>2</sub>TPPBr with diethyl phosphite in the presence of the copper iodide/*N,N'*-dimethyldiaminoethane (L) catalytic system and cesium carbonate as a base was studied (Scheme 1). This catalytic system



Scheme 1. Cu-mediated phosphorylation of ZnTPPBr.

developed by Buchwald et al.<sup>[65]</sup> has been previously successfully used to prepare *meso*-(dialkoxyphosphoryl)porphyrins from the corresponding *meso*-iodo-substituted derivatives.<sup>[21]</sup> H<sub>2</sub>TPPBr was initially transformed into the zinc porphyrinate ZnTPPBr by a standard metallation procedure to avoid porphyrin metallation by copper iodide under the phosphorylation reaction conditions.

When ZnTPPBr was treated with diethyl phosphite in the presence of 20 mol% of CuI, 1.5 equivalents of diamine L and an excess of Cs<sub>2</sub>CO<sub>3</sub>, only traces of the desirable product **1Zn** were detected by MALDI-TOF mass spectrometry even after two days (Scheme 1), Table 1, entry 1). Product **1Zn** was obtained in higher yield (35%) when a stoichiometric amount of copper iodide and seven equivalents of the diamine L were used (Table 1, entry 2). The amount of the base has only a negligible effect on the reaction outcome (Table 1, entry 3), but an excess of diethyl phosphite leads to a higher reaction yield (Table 1, entries 2–4). However, it has to be noted that the conversion of ZnTPPBr and the reaction yield were still moderate when twelve equivalents of the reagent was used (Table 1, entry 4). It is noteworthy that the presence of the diamine L is a key factor for the reaction course, because no product was detected by MALDI-TOF mass spectrometry of the reaction mixture in the absence of the amine L (Table 1, entry 5). By using the same conditions, di-*n*-butyl phosphite was more reactive and the corresponding phosphonate **2Zn** was obtained in 50% yield, whereas diethyl phosphite afforded the product **1Zn** in 35%

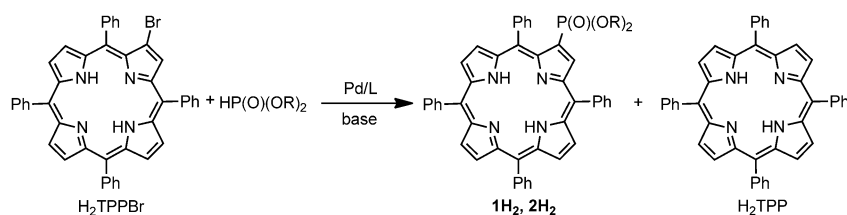
Table 1. Copper-mediated phosphorylation of ZnTPPBr with dialkyl phosphites.<sup>[a]</sup>

	HP(O)(OR) <sub>2</sub> [equiv] (R)	CuI [equiv]	L [equiv]	Cs <sub>2</sub> CO <sub>3</sub> [equiv]	Conv [%] <sup>[b]</sup>	Product	Yield [%] <sup>[c]</sup>
1	3 (Et)	0.2	1.5	7	5 (95)	<b>1Zn</b>	< 5 <sup>[d]</sup>
2	6 (Et)	1	7	7	35 (65)	<b>1Zn</b>	35
3	3 (Et)	1	7	35	25 (74)	<b>1Zn</b>	24
4	12 (Et)	1	7	16	50 (49)	<b>1Zn</b>	44
5	24 (Et)	1	–	7	0	<b>1Zn</b>	0 <sup>[d]</sup>
7	3 ( <i>n</i> Bu)	1	7	7	50 (49)	<b>2Zn</b>	50
8	24 ( <i>n</i> Bu)	3	21	14	100 (0)	<b>2Zn</b>	94
9	24 ( <i>i</i> Pr)	3	21	14	100 (0)	<b>3Zn</b>	86
10	24 ( <i>t</i> Bu)	3	21	14	0	<b>4Zn</b>	0 <sup>[d]</sup>

[a] Reaction conditions: ZnTPPBr (0.02–0.04 mmol each), HP(O)(OR)<sub>2</sub>, CuI, L, and Cs<sub>2</sub>CO<sub>3</sub> were heated to reflux in toluene (3 mL) for two days under N<sub>2</sub>. [b] Conversion was estimated by <sup>1</sup>H NMR spectroscopic analysis of the crude reaction mixture; yields of isolated starting material ZnTPPBr are given in brackets. [c] Yields of isolated product. [d] Yield estimated by <sup>1</sup>H NMR spectroscopic analysis of the crude reaction mixture.

yield (Table 1, entries 2 and 7). Full conversion of the starting material ZnTPPBr was observed when the amount of all reagents was increased up to 24 equivalents of di-*n*-butyl phosphite, 14 equivalents of Cs<sub>2</sub>CO<sub>3</sub>, three equivalents of CuI, and 21 equivalents of the amine L (Table 1, entry 8). Under these conditions the yield of the isolated target product **2Zn** was 94%. A high yield (86%) of the phosphonate was also obtained when ZnTPPBr was reacted with di-*iso*-propyl phosphite (Table 1, entry 9), however, sterically hindered di-*tert*-butyl phosphite did not react under these conditions (Table 1, entry 10).

Next, we set out to develop conditions for the palladium-catalyzed formation of β-diethoxyphosphoryl derivatives (Scheme 2). It has previously been shown that the Pd-catalyzed carbon–phosphorous bond-forming reaction is efficient for the synthesis of *meso*-bis(diethoxyphosphoryl)porphyrins.<sup>[26,27]</sup>



Scheme 2. Pd-mediated phosphorylation of H<sub>2</sub>TPPBr.

The obtained results are summarized in Table 2. Interestingly, the reactivity of H<sub>2</sub>TPPBr and ZnTPPBr in the presence of palladium catalysts was different compared to *meso*-dibromoporphyrins. Ethanol was found to be the best solvent for the reaction of *meso*-dibromoporphyrins with diethyl phosphite in the presence of a [Pd(OAc)<sub>2</sub>/3 PPh<sub>3</sub>] catalytic system and NEt<sub>3</sub>. When H<sub>2</sub>TPPBr was reacted with diethyl phosphite under the same conditions, the yield of the target product **1H<sub>2</sub>** was very low even in the presence of stoichio-

Table 2. Pd-mediated phosphorylation of H<sub>2</sub>TPPBr with diethyl phosphite.<sup>[a]</sup>

	Base	[Pd]/L ([equiv])	Conv [%] <sup>[b]</sup>	Yield [%] <sup>[c]</sup>	
				<b>1H<sub>2</sub></b>	H <sub>2</sub> TPP
1 <sup>[d]</sup>	NEt <sub>3</sub>	Pd(OAc) <sub>2</sub> /3 PPh <sub>3</sub> (1)	10	5 <sup>[e]</sup>	5 <sup>[e]</sup>
2	NEt <sub>3</sub>	Pd(OAc) <sub>2</sub> /3 PPh <sub>3</sub> (1)	100	87	11
3	N( <i>i</i> Pr) <sub>2</sub> Et	Pd(OAc) <sub>2</sub> /3 PPh <sub>3</sub> (1)	100	84 <sup>[e]</sup>	16 <sup>[e]</sup>
4	NCy <sub>2</sub> Me <sup>[f]</sup>	Pd(OAc) <sub>2</sub> /3 PPh <sub>3</sub> (1)	100	63 <sup>[e]</sup>	37 <sup>[e]</sup>
5	N( <i>i</i> Pr) <sub>2</sub> Et	Pd(OAc) <sub>2</sub> /2 dppf <sup>[g]</sup> (1)	100	70 <sup>[e]</sup>	30 <sup>[e]</sup>
6	N( <i>i</i> Pr) <sub>2</sub> Et	Pd(OAc) <sub>2</sub> /2 BINAP <sup>[h]</sup> (1)	0	–	–
7	NEt <sub>3</sub>	Pd(OAc) <sub>2</sub> /3 PPh <sub>3</sub> (0.5)	50	35	5
8	NEt <sub>3</sub>	[Pd(PPh <sub>3</sub> ) <sub>4</sub> ] (0.5)	90	84	6
9	NEt <sub>3</sub>	[Pd(PPh <sub>3</sub> ) <sub>4</sub> ] (0.25)	79	72	5 <sup>[i]</sup>
10 <sup>[j]</sup>	NEt <sub>3</sub>	[Pd(PPh <sub>3</sub> ) <sub>4</sub> ] (0.15)	70	43	20 <sup>[j]</sup>

[a] Reaction conditions: H<sub>2</sub>TPPBr (0.03 mmol), HP(O)(OEt)<sub>2</sub> (12 equiv), [Pd]/L, and the base (15 equiv) were heated to reflux in toluene (3 mL) for two days under N<sub>2</sub>. [b] Conversion estimated by <sup>1</sup>H NMR spectroscopic analysis of the crude reaction mixture. [c] Yield of isolated product. [d] Ethanol was used as a solvent. [e] <sup>1</sup>H NMR spectroscopic yield according to the crude reaction mixture analysis. [f] Cy = cyclohexyl. [g] Dppf = 1,1'-bis(diphenylphosphino)ferrocene. [h] BINAP = 2,2'-bis(diphenylphosphino)-1,1'-bi-naphthyl. [i] Yield determined by <sup>1</sup>H NMR spectroscopy of the isolated mixture of H<sub>2</sub>TPPBr and H<sub>2</sub>TPP. [j] 25 equivalents of HP(O)(OEt)<sub>2</sub> and 30 equivalents of NEt<sub>3</sub> were also tested and gave similar results.

metric amounts of the catalytic system (Table 2, entry 1). This can be attributed to the low solubility of H<sub>2</sub>TPPBr in ethanol. Further investigations proved toluene to be a good reaction solvent. Full conversion of H<sub>2</sub>TPPBr was achieved after two days in the presence of one equivalent of [Pd(OAc)<sub>2</sub>/3 PPh<sub>3</sub>] when a large excess of diethyl phosphite (12 equiv) and NEt<sub>3</sub> (15 equiv) was used (Table 2, entry 2). The product **1H<sub>2</sub>** was isolated in 87% yield, H<sub>2</sub>TPP being the only byproduct. A number of amines and ligands was tested in order to avoid the hydrodebromination side reaction leading to the formation of H<sub>2</sub>TPP, however none of them were superior to the first examined system (Table 2, entries 3–6). When H<sub>2</sub>TPPBr was reacted with di-*n*-butyl phosphite under the optimal conditions (Table 2, entry 2), full conversion of the starting bromide was observed and the target product **2H<sub>2</sub>** was isolated in 92% yield.

Further, catalytic conditions were studied to perform the coupling of H<sub>2</sub>TPPBr with diethyl phosphite. Decreasing the amount of [Pd(OAc)<sub>2</sub>/3 PPh<sub>3</sub>] led to an incomplete conversion of the starting bromide (Table 2, entry 7). It should be noted that [Pd(PPh<sub>3</sub>)<sub>4</sub>] was more efficient (Table 2, entries 8 and 9) and the product was obtained in 72% yield by using 25 mol% of this catalyst. Further decrease in the catalyst loading to 15 mol% led to an incomplete conversion of H<sub>2</sub>TPPBr (Table 2, entry 10) and a significant increase of by-product formation (H<sub>2</sub>TPP), even when the reaction was carried out in the presence of 25 equivalents of diethyl phos-

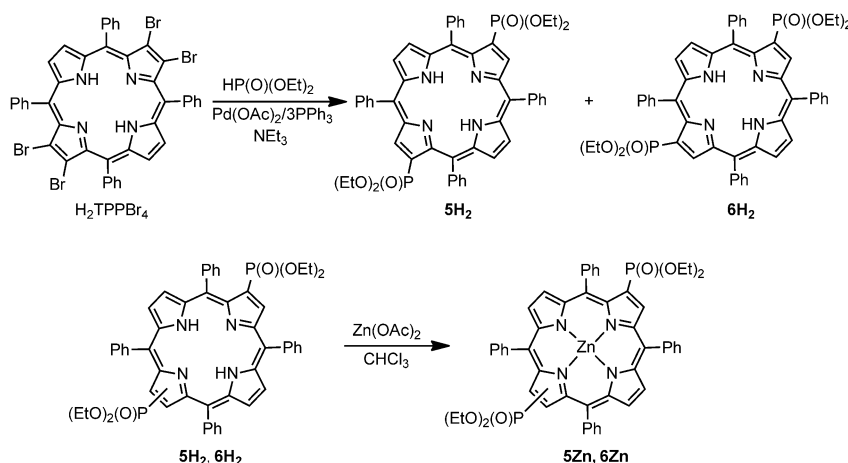
phite (Table 2, entry 9). The potential metallation of  $H_2TPPBr$  by palladium complexes can be excluded according to MALDI-TOF mass spectrometry data. The low catalyst efficiency can be explained by the formation of catalytically inactive palladium complexes containing diethyl phosphite as a ligand,<sup>[66]</sup> however, the attempts to perform the reaction in the presence of smaller amounts of diethyl phosphite (1.2 equiv) and  $NEt_3$  (1.5 equiv) were unsuccessful. The low  $H_2TPPBr$  conversion observed under these conditions shows that the carbon-phosphorous bond formation is slow when diethyl phosphite is used in small excess.

It was expected that  $ZnTPPBr$  would be more reactive compared to  $H_2TPPBr$  as has been observed in the reactions of *meso*-dibromoporphyrins.<sup>[26]</sup> In fact, their reactivity is similar and full conversion of the starting bromide was observed only in the presence of a stoichiometric amount of  $[Pd(OAc)_2/3PPh_3]$  or 0.5 equivalents of  $[Pd(PPh_3)_4]$  and a large excess of diethyl phosphite (12 equiv) and triethylamine (15 equiv). Moreover, the product purification by column chromatography was more difficult due to the coordination of triphenylphosphine oxide formed during the reaction to porphyrinatozinc **1Zn**. In this case, an additional demetallation step was required to obtain the pure product **1H<sub>2</sub>**.

The developed conditions for the Pd-catalyzed C–P bond-forming reaction were further applied to the synthesis of  $\beta$ -poly(dialkoxylphosphoryl)porphyrins. 2,3,12,13-Tetrabromo-5,10,15,20-tetraphenylporphyrin ( $H_2TPPBr_4$ ), was readily prepared through controlled bromination of  $H_2TPP$  with *N*-bromosuccinimide.<sup>[62]</sup> When  $H_2TPPBr_4$  was reacted with diethyl phosphite by using the conditions optimized for  $H_2TPPBr$  (Table 2, entry 2), the starting material and a complex mixture of products were observed according to MALDI-TOF mass spectrometry. However, the products formed in the course of the stepwise phosphorylation of  $H_2TPPBr_4$  (e.g.,  $H_2TPP(X)Br_3$ ,  $H_2TPP(X)_2Br_2$ ,  $H_2TPP(X)_3Br$ , where  $X=P(O)(OEt)_2$ ) were not observed indicating that the dibromopyrrole moiety did not directly react with diethyl phosphite. It is possible to assume that the phosphorylation reaction takes place only after the reduction of one of the neighboring bromine atoms leading to the formation of a mono- $\beta$ -diethoxyphosphoryl-substituted pyrrole moiety. This distinguishes the developed transformation from the previously described Pd-catalyzed  $\beta$ -functionalization reactions, where both of the bromine atoms get substituted with the used nucleophile.<sup>[67]</sup>

A controlled one-pot reaction involving consecutive reduction and phosphorylation of  $H_2TPPBr_4$  would provide an

easy approach to the unknown 2,12(13)-bis(diethoxyphosphoryl)porphyrins **5H<sub>2</sub>** and **6H<sub>2</sub>**. These compounds cannot be obtained by direct metal-mediated C–P bond-forming reactions, because the corresponding  $\beta$ -dibromoporphyrins are not available by selective dibromination of  $H_2TPP$ . Therefore, we set out to develop conditions for the selective synthesis of the bis(phosphoryl) porphyrins **5H<sub>2</sub>** and **6H<sub>2</sub>** starting from  $H_2TPPBr_4$  (Scheme 3). Extending the reaction time, raising the amounts of diethyl phosphite and  $NEt_3$ , as



Scheme 3. Synthesis of 2,12(13)-bis(diethoxyphosphoryl)porphyrins **5H<sub>2</sub>**, **6H<sub>2</sub>**, **5Zn**, and **6Zn**.

well as by using two equivalents of palladium acetate, led to complex mixtures of products, whereas the conversion did not exceed 50%. Low conversions were also observed when toluene was replaced by THF or ethanol. Although no phosphorylated products were observed in the reaction mixtures by MALDI-TOF mass spectrometry, the use of ethanol as the solvent did promote the reduction step of the sequence. Thus, a mixture of toluene and ethanol was used to increase the solubility of the porphyrin, to facilitate the reduction, and to allow the consecutive phosphorylation of the resulting bromoporphyrins (Table 3).

Interestingly, the ratio of the solvents was a key parameter influencing the conversion and the yields of the bis(phosphoryl)porphyrins **5H<sub>2</sub>** and **6H<sub>2</sub>** (Table 3, entries 1–4). The best result was observed when ethanol and toluene were used in a 2:3 ratio (Table 3, entry 3). By using these conditions, the bis(phosphoryl)porphyrins **5H<sub>2</sub>** and **6H<sub>2</sub>** were obtained in equal amounts with a total yield of 81%. Both increasing and decreasing of ethanol content led to an incomplete reaction and lower yields of the target products (Table 3, entries 2 and 4). When the amount of  $[Pd(OAc)_2/3PPh_3]$  was decreased twice, the conversion of  $H_2TPPBr_4$  was still complete but the target products **5H<sub>2</sub>** and **6H<sub>2</sub>** were obtained in a slightly lower yield (68%). The separation of the regioisomers **5H<sub>2</sub>** and **6H<sub>2</sub>** by column chromatography was quite delicate. However, the corresponding porphyrinatozinc complexes **5Zn** and **6Zn**, easily obtained by metallation of the mixture of **5H<sub>2</sub>** and **6H<sub>2</sub>** (Scheme 3), were separated

Table 3. Pd-mediated phosphorylation of H<sub>2</sub>TPPBr<sub>4</sub> with diethyl phosphite.<sup>[a]</sup>

	Ethanol/Toluene	Conv [%] <sup>[b]</sup>	Yield [%] <sup>[c]</sup>		
			5H <sub>2</sub> , 6H <sub>2</sub> <sup>[d]</sup>	1H <sub>2</sub>	H <sub>2</sub> TPP
1	5:95	<25 <sup>[e]</sup>	n/i <sup>[f]</sup>	n/i	n/i
2	25:75	70	10	n/i <sup>[g]</sup>	25
3	40:60	100	81	17	<2
4	50:50	60	20	15	20
5 <sup>[h]</sup>	40:60	100	68	21	6

[a] Reaction conditions: H<sub>2</sub>TPPBr<sub>4</sub> (0.01–0.04 mmol), HP(O)(OEt)<sub>2</sub> (12 equiv), [Pd(OAc)<sub>2</sub>/3PPh<sub>3</sub>] (1 equiv), and NEt<sub>3</sub> (15 equiv) were heated to reflux in the solvent mixtures (3 mL) for two days under N<sub>2</sub>. [b] Conversion was estimated by <sup>1</sup>H NMR spectroscopy. [c] Yield of isolated product. [d] The regioisomers of 5H<sub>2</sub> and 6H<sub>2</sub> were obtained in equal amounts in all the reactions. [e] A complex mixture of products containing 5H<sub>2</sub>, 6H<sub>2</sub>, 1H<sub>2</sub>, mono- and dibromo-substituted derivatives of 1H<sub>2</sub> and H<sub>2</sub>TPP according to MALDI-TOF mass spectrometry was obtained. [f] n/i not isolated [g] A complex mixture of products containing 1H<sub>2</sub> bromo-substituted derivatives according to MALDI-TOF mass spectrometry was obtained. [h] 0.5 equivalents of [Pd(OAc)<sub>2</sub>/3PPh<sub>3</sub>] were used.

rated by column chromatography on silica gel by using CH<sub>2</sub>Cl<sub>2</sub>/MeOH (99:1) as eluent.

To get some insight into the reaction course, H<sub>2</sub>TPPBr<sub>4</sub> was reacted with diethyl phosphite in the presence of NEt<sub>3</sub> without the Pd catalyst. Partial reduction of the *gem*-dibromoalkenes to the bromoalkenes is possible under these conditions.<sup>[68,69]</sup> Recently, a one-pot reaction including consecutive reduction and copper-mediated phosphorylation reactions of *gem*-dibromoalkenes was described.<sup>[70]</sup> However, the reaction did not proceed when H<sub>2</sub>TPPBr<sub>4</sub> was heated to reflux with diethyl phosphite and NEt<sub>3</sub> in the ethanol/toluene mixture (2:3) for two days. Thus, both ethanol and a palladium catalyst are needed to achieve the H<sub>2</sub>TPPBr<sub>4</sub> reduction. Moreover, H<sub>2</sub>TPPBr<sub>4</sub> does not react with diethyl phosphite directly, because tri- and tetra-diethoxyphosphoryl-substituted porphyrins were never observed in the reaction mixtures by MALDI-TOF mass spectrometry. Therefore, the Pd-catalyzed hydrodebromination reaction of H<sub>2</sub>TPPBr<sub>4</sub> probably leads to the formation of partially reduced products, which then participate in consecutive C–P bond-forming reactions giving 5H<sub>2</sub> and 6H<sub>2</sub> along with 1H<sub>2</sub> and H<sub>2</sub>TPP.

**Crystal structures of the zinc β-phosphoryl porphyrins 1Zn and 3Zn:** Single crystals of complexes 1Zn and 3Zn were grown by slow evaporation of methanol/benzene and methanol/CHCl<sub>3</sub>/heptane mixtures, respectively, and their structures were elucidated by X-ray crystallography. According to the X-ray diffraction data, both complexes are zinc β-mono-phosphorylporphyrinate cofacial dimers formed by two P–O⋯Zn coordination bonds (Figures 1 and 2). The zinc atom is located within the center of the porphyrin ring (Zn–N 2.047(8)–2.076(8) Å in 1Zn, Zn–N 2.061(4)–2.083(5) Å in 3Zn) and the fifth position in the tetragonal-pyramidal environment of the Zn atom is occupied by one oxygen atom of the phosphoryl substituent of the adjacent porphyrin molecule (Zn–O 2.086(7) Å for 1Zn and 2.098(4) Å for 3Zn). Two cofacial porphyrin molecules are

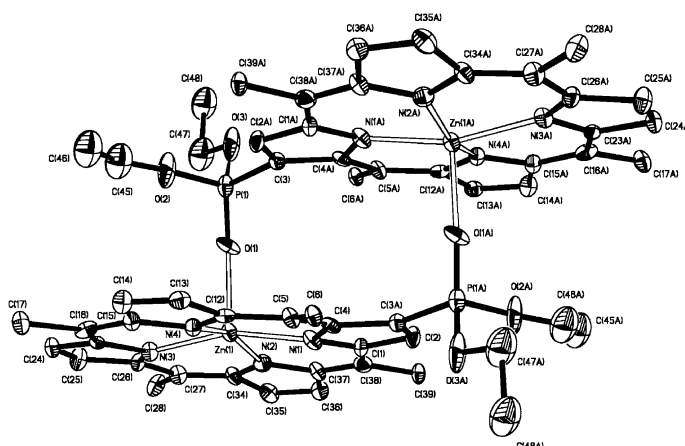


Figure 1. Molecular structure of 1Zn (30% probability ellipsoids). Hydrogen atoms and phenyl groups are omitted for clarity.

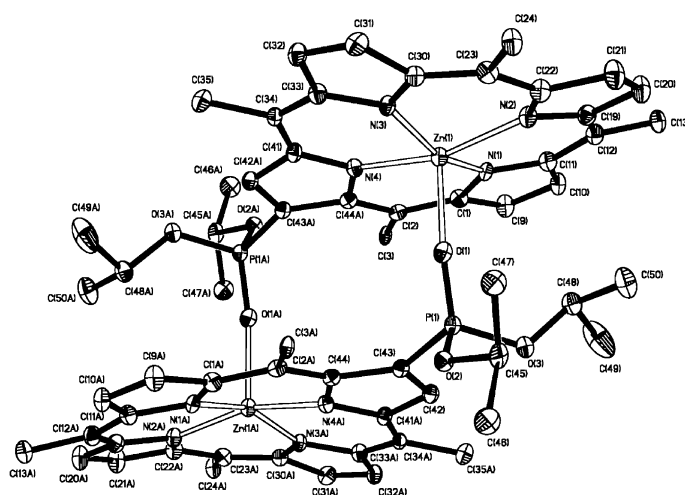


Figure 2. Molecular structure of 3Zn (30% probability ellipsoids). Hydrogen atoms and phenyl groups are omitted for clarity.

partially overlapped. As a result each phosphoryl-substituted pyrrole fragment is located above the second porphyrin core. Significant difference in the dimer geometry was observed for compound 3Zn compared to 1Zn, which possesses the less-bulky ethoxy substituents at the phosphoryl group. The distance between two porphyrin N<sub>4</sub> planes is significantly different and is equal to 3.90 and 4.51 Å in 1Zn and 3Zn, respectively. Moreover, displacement of the zinc atom from the porphyrin N<sub>4</sub> plane increases by 0.067 Å. The P–O–Zn angle varies from 147.9(5) to 160.2(2)° and the O(1)–P(1)–C angle changes from 116.3(5) to 106.0(2)° for 1Zn and 3Zn, respectively. Relatively short contacts (3.4–3.7 Å) were observed between the carbon atoms of the *iso*-propoxy substituents and the atoms of the closest pyrrole ring of the adjacent porphyrin macrocycle in the dimer of 3Zn. These contacts give rise to a decrease in the angle between the Zn(1A)–N(1A) line and the Zn(1A)O(1A)P(1A) plane from 22.5° in 1Zn to 16.1° in 3Zn. At the same time, the Zn⋯P distance in 3Zn (3.520 Å) increases compared to

**1Zn** (3.413 Å). Two benzene molecules are present in the crystal structure of **1Zn**, methanol and water molecules—in **3Zn**. It is interesting to note that in both cases the solvent molecules do not have any contacts with the porphyrin dimers.

Matano and co-workers have reported similar dimers formed by mono-substituted *meso*-dialkoxyphosphorylporphyrin and 5-di-*n*-butoxyphosphoryl-10,15,20-tris(3,5-di-*tert*-butylphenyl)porphyrinatozinc(II) (*meso*-monoPZn) (Figure 3).<sup>[21]</sup> Moreover, it was previously shown by us that

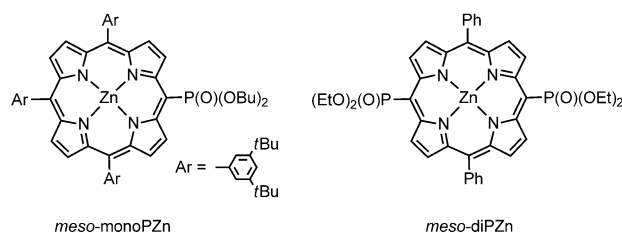


Figure 3. Structures of *meso*-monoPZn and *meso*-diPZn.

self-assembling of 5,15-bis(diethoxyphosphoryl)-10,20-diphenylporphyrinatozinc(II) (*meso*-diPZn) (Figure 3) led to a 2D coordination polymer formed by interconnection of the porphyrinatozinc(II) units through the coordination of the Zn centers by two phosphoryl groups belonging to two adjacent molecules.<sup>[26]</sup> Selected structural parameters of four phosphoryl porphyrin derivatives are summarized in Table 4. A number of the parameters are similar for the  $\beta$ - and the *meso*-substituted porphyrin dimers **1Zn**, **2Zn**, and *meso*-monoPZn despite the different location of the dialkoxy-

Table 4. Selected bond lengths [Å] and angles [°] of four (dialkoxyphosphoryl)porphyrinato zinc complexes.

	<b>1Zn</b> <sup>[a]</sup>	<b>3Zn</b> <sup>[a]</sup>	<i>meso</i> -monoPZn <sup>[b]</sup>	<i>meso</i> -diPZn <sup>[c]</sup>
Zn(1)–O(1)	2.086(7)	2.098(4)	2.102(3)	2.465(2)
P(1)–O(1)	1.460(7)	1.474(4)	1.478(3)	1.473(3)
P(1)–O(2) <sup>[d]</sup>	1.494(11) <sup>[d]</sup>	1.561(4)	1.579(3)	1.574(3)
P(1)–O(3)	1.561(8)	1.577(4)	1.580(4)	1.583(3)
Zn–plane N <sub>4</sub>	0.317	0.384	0.331	–
Zn–porphyrin N <sub>4</sub> plane	0.0006	0.028	0.0086	–
N <sub>4</sub> –N <sub>4</sub> planes	3.90	4.51	3.04	–
Zn···Zn	7.187	7.336	6.253	–
Zn···P	3.413	3.520	3.296	–
Zn(1)–O(1)–P(1)	147.9(5)	160.2(2)	133.4(2)	158.20(15)
O(1)–P(1)–O(2) <sup>[d]</sup>	110.5(6)	115.7(2)	108.1(2)	112.99(15)
O(1)–P(1)–O(3)	115.3(4)	113.2(2)	111.9(2)	113.95(16)
O(2)–P(1)–O(3) <sup>[e]</sup>	106.3(6)	102.7(2)	105.97(19)	100.58(15)
O(1)–P(1)–C	116.3(5)	106.0(2)	–	–
Zn–N(C)/ZnPO angle Ph/N <sub>4</sub>	22.5	16.1	–	–
	99.9	96.9	119.7 <sup>[e]</sup>	–
	64.4	75.8	103.3	–
	66.7	73.9	94.4	–
	58.4	63.5	–	–

[a] Data from this work. [b] Data from reference [21]. [c] Data from reference [26]. [d] The [OEt] fragment (O(2), C(45), C(46)) in **1Zn** is disordered at practically the same sites. [e] 3,5-Di-*tert*-butylphenyl substituents.

phosphoryl group on the porphyrin core. The Zn<sup>II</sup> atom adopts a distorted tetragonal-pyramidal coordination geometry. Displacement of the five-coordinated zinc ion from the mean porphyrin N<sub>4</sub> plane in **1Zn** (0.317 Å) and in **3Zn** (0.384 Å), is similar to that observed in *meso*-monoPZn (0.331 Å) but the average deviation of the nitrogen atoms from the porphyrin plane varies from an almost flat arrangement in **1Zn** and *meso*-monoPZn (deviation from the N<sub>4</sub> plane is 0.001 and 0.009 Å, respectively) up to 0.028 Å in the sterically hindered **3Zn**. In contrast, the Zn atoms are located exactly in the center of the porphyrin ring in the 2D coordination network formed by *meso*-diPZn. The Zn···O=P distances are similar for the three dimers (2.086(7), 2.098(4), and 2.102(3) Å, respectively) and are significantly longer in the 2D polymer (2.465(2) Å). It should be noted, that the interplanar distance between the two porphyrin N<sub>4</sub> planes in the dimer increases from 3.04 to 3.90 Å when the position of the diethoxyphosphoryl substituent is changed from *meso* to  $\beta$  at the porphyrin core, and further increases up to 4.51 Å in the more sterically hindered compound **3Zn**. The Zn–Zn distance changes in the same order (6.253, 7.187, and 7.336 Å, respectively). Considering the value of these two parameters, Matano and co-workers have proposed the *meso*-monoPZn dimer as a new model for a weakly coupled chlorophyll pair in the photosynthetic reaction center.<sup>[21]</sup> Indeed, in the special pair P700 formed by two chlorophylls in photosystem I (PSI) the metal separation is equal to 6.3 Å and differs from the special pair formed by the bacteriochlorophylls in the purple bacterial reaction center (PbRC),<sup>[71]</sup> where the Mg<sup>II</sup> separation is larger (7.6 Å).<sup>[72]</sup>

Thus,  $\beta$ -dialkoxyphosphorylporphyrins can be regarded as model compounds for the weakly coupled chlorophyll pairs in photosynthesis as well as *meso*-monoPZn. Moreover, the functional group is located at the  $\beta$ -position in these compounds as in the naturally occurring chlorophyll. The metal–metal separation and interplanar porphyrin distance can be tuned by changing the size and the position of the alkoxy substituents of the phosphoryl group as it was shown above for **1Zn**, **3Zn**, and *meso*-monoPZn.

**IR studies:** Infrared spectroscopy was used to get insight into the structures of **2Zn**, **5Zn**, and **6Zn** in the solid state. It was shown that the position of the P=O stretching vibration band, which is observed in the region of  $\tilde{\nu}$  = 1180–1280 cm<sup>-1</sup> of the IR spectrum reflects the formation of P=O···Zn coordination bonds involving adjacent porphyrin molecules. In the IR spectra of the self-assembling zinc porphyrinates, these vibration bands were observed at lower frequencies ( $\Delta\tilde{\nu}$  = 7–30 cm<sup>-1</sup>) than those of the corresponding free-base porphyrins.<sup>[26]</sup> Moreover, two distinct vibrations at  $\tilde{\nu}$  = 1259 and 1233 cm<sup>-1</sup> were detected in powder samples of the 2D coordination polymer of *meso*-diPZn. The vibration frequency of the first one was similar to the P=O band of 5,15-bis(diethoxyphosphoryl)-10,20-diphenylporphyrin ( $\tilde{\nu}$  = 1250 cm<sup>-1</sup>) and was assigned to the vibration of an uncoordinated peripheral phosphoryl group. The second band was attributed to the vibration of a coordinated

phosphoryl group  $\text{P}=\text{O}\cdots\text{Zn}$ , because only this band was observed in the IR spectrum of a monocrystalline solid sample of the 2D coordination polymer of *meso*-diPZn.

In accordance with this data and the X-ray diffraction data on a single crystal, a strong  $\text{P}=\text{O}$  stretching vibration band of **1Zn** ( $\tilde{\nu}=1228\text{ cm}^{-1}$ ) was observed at lower frequencies than the corresponding band in the free-base porphyrin **1H<sub>2</sub>** ( $\tilde{\nu}=1245\text{ cm}^{-1}$ ). Only one  $\nu(\text{P}=\text{O})$  band at  $\tilde{\nu}=1213\text{ cm}^{-1}$  corresponding to the vibration of a coordinated phosphoryl group, was observed in the spectrum of **3Zn**, reflecting a molecular self-assembling through  $\text{P}=\text{O}\cdots\text{Zn}$  interactions in the solid state. A similar frequency shift of the  $\text{P}=\text{O}$  bands was observed for the solid state IR spectra of **2Zn** ( $\tilde{\nu}=1220\text{ cm}^{-1}$ ) and **2H<sub>2</sub>** ( $\tilde{\nu}=1250\text{ cm}^{-1}$ ). Thus, the interconnection of Zn centers by the di-*n*-butoxyphosphoryl group also exists in the solid state samples of **2Zn**. Taking into account the structural similarity of **1Zn**, **2Zn**, and **3Zn**, formation of cofacial dimers seems to be the most probable pathway for the self-organization of **2Zn** in the solid state. Vibrations of coordinated phosphoryl groups observed in the spectra of **5Zn** and **6Zn** ( $\tilde{\nu}=1232$  and  $1240\text{ cm}^{-1}$ , respectively) are very similar to those observed for the 2D coordination polymer of *meso*-diPZn ( $\tilde{\nu}=1232\text{ cm}^{-1}$ ).

**Association in solution:** Association of porphyrins **1Zn** and **3Zn** in solution was first investigated by UV/Vis spectroscopy in toluene and chloroform. As expected, the UV/Vis spectra of the free-base porphyrins **1H<sub>2</sub>** and **2H<sub>2</sub>** are not concentration dependent. Figure 4 shows the concentration dependence of the absorption spectrum of the metalloporphyrin **1Zn** in toluene. Increasing the concentration of **1Zn** leads to a bathochromic shift and broadening of all the porphyrin bands in the spectrum. The Soret band shifts only by 3 nm when the **1Zn** concentration increases from  $1.4\times 10^{-5}$  to  $3.6\times 10^{-4}\text{ M}$ . The Q-band shifts are observable at higher concentrations due to the lower intensity of these bands. Again, significant shifts (from  $\lambda=557$  up to 569 nm,  $\Delta\lambda=12\text{ nm}$  and from  $\lambda=596$  up to 612 nm,  $\Delta\lambda=16\text{ nm}$ ) were detected when the compound concentration was increased from  $1.8\times 10^{-5}$  to  $1.4\times 10^{-3}\text{ M}$  indicating that molecular association takes place at this concentration range.

Consequently, UV/Vis absorption spectroscopy can be used to estimate more precisely the concentration limits where self-association of compound **1Zn** takes place. Indeed, an expected linear evolution of the intensity of the Soret band ( $\lambda=429\text{ nm}$ ) occurs in the concentration range of  $1\times 10^{-7}$ – $5\times 10^{-5}\text{ M}$  (see the Supporting Information, Figure S1). A significant deviation from the law of Lambert is observed only for concentrations of **1Zn** higher than  $5\times 10^{-5}\text{ M}$ , whereas the bathochromic shift of all porphyrin bands is observed. Increasing the concentration of **1Zn** in chloroform does not lead to the bathochromic shift of the Soret band ( $\lambda=430\text{ nm}$ ). However, the deviation from the law of Lambert is observed when the concentration of the compound is higher than  $1\times 10^{-4}\text{ M}$  (see the Supporting Information, Figure S2).

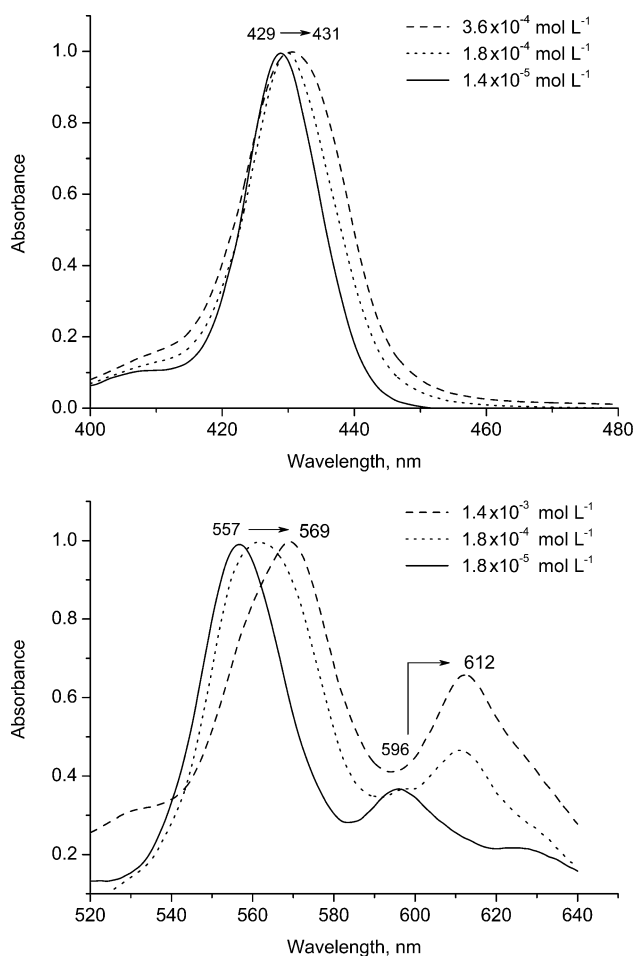


Figure 4. UV/Vis absorption spectra of **1Zn** in toluene at different concentrations. The spectra are normalized for comparison.

Molecular association of **3Zn** in toluene also induced bathochromic shifts of the Q-bands and the broadening of the Soret band (see the Supporting Information, Figure S3). The nature of the alkyl substituents located on the phosphoryl group does not significantly influence the concentration limits of the association process. The law of Lambert is observed at concentrations lower than  $5\times 10^{-5}\text{ M}$  in toluene and  $1\times 10^{-4}\text{ M}$  in chloroform for **1Zn** and **3Zn**.

**<sup>1</sup>H and <sup>31</sup>P{<sup>1</sup>H} NMR spectroscopic studies:** The <sup>1</sup>H NMR spectra of the free-base porphyrins **1H<sub>2</sub>** and **3H<sub>2</sub>** in CDCl<sub>3</sub> reveal the expected resonances of all the protons (<sup>1</sup>H NMR spectrum for **1H<sub>2</sub>** shown as an example, see the Supporting Information, Figure S4). In contrast, the <sup>1</sup>H NMR spectrum of **1Zn** in CDCl<sub>3</sub> ( $10^{-2}$ – $10^{-4}\text{ M}$ ) at 303 K consists of a broad, poorly resolved set of signals, which prevents the structure determination (Figure 5). However, a well-resolved spectrum could be obtained after the addition of 30% v/v of [D<sub>4</sub>]MeOH (Figure 5). In this spectrum all the expected proton signals are observed, but some of the phenylic and pyrrolic protons occasionally overlap. The downfield doublet ( $\delta=9.5\text{ ppm}$ ) was attributed to the proton of the P<sup>1</sup> fragment (see Figure 6 for the proton numbering). Resonances

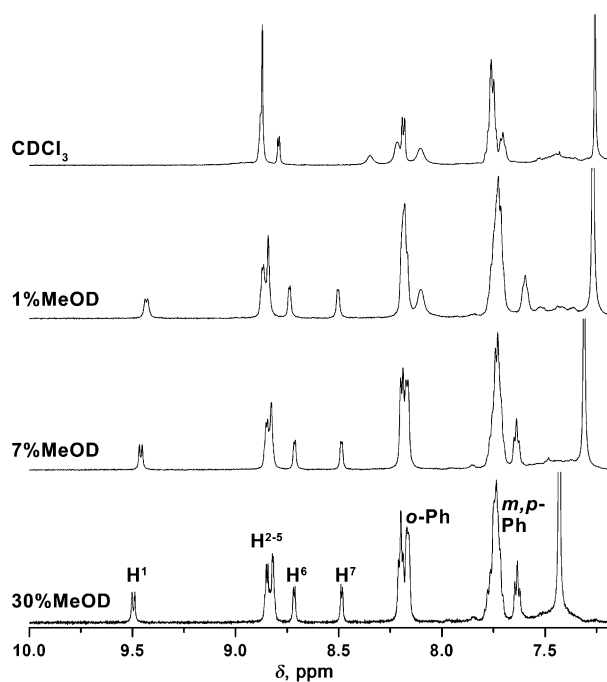


Figure 5. Aromatic region of the  $^1\text{H}$  NMR spectra of **1Zn** in  $\text{CDCl}_3$  ( $10^{-3}\text{M}$ ) at 303 K before and after the addition of different amounts of  $[\text{D}_4]\text{MeOH}$ .

of the  $\text{P}^2$  and  $\text{P}^3$  pyrrolic protons are observed as broadened singlets at  $\delta \approx 8.8$  ppm. In contrast, the protons of the  $\text{P}^4$  fragment appear as two doublets with significantly different chemical shifts. The resonances of the  $\text{P}^{4(7)}$  protons are shifted upfield due to the ring current effects of the sterically hindered phenyl substituent  $\text{Ph}^1$ . It is important to note that the most significant variation in the chemical shifts of the pyrrolic protons and the line widths of the alkoxy groups were observed after the addition of only trace amounts of  $[\text{D}_4]\text{MeOH}$  (1% v/v). The observed influence of methanol on the spectrum of **1Zn** allows to conclude that weak molecular aggregates are formed in  $\text{CDCl}_3$ , presumably through coordination of the diethoxyphosphoryl groups to the metal centers. Indeed, methanol can replace the axially coordinated  $\text{P}(\text{O})(\text{OEt})_2$  groups in the molecular aggregates favoring the formation of the monomeric **1Zn** form.

The association of **3Zn** in  $\text{CDCl}_3$  is weaker than that of **1Zn** and the proton resonances of **3Zn** are only slightly broadened at room temperature (see the Supporting Information, Figure S5). Sharp resonances of all aromatic protons were observed after the addition of only  $5\ \mu\text{L}$  ( $\approx 1\%$  v/v) of  $[\text{D}_4]\text{MeOH}$ . Under these conditions, the chemical shifts of all protons are similar to those observed in pure  $\text{CDCl}_3$ .

Variable-temperature NMR (VT-NMR) studies (223–323 K) of solutions of **1Zn** and **3Zn** in  $[\text{D}]\text{chloroform}$  and  $[\text{D}_8]\text{toluene}$  provided additional information about the structure of the aggregates in solution (see the Supporting Information, Table S1). Schematic representations of possible structures of the associates are shown in Figure 6. Besides the dimeric species, which were obtained in the solid state (Figure 6A), at least two other supramolecular associates

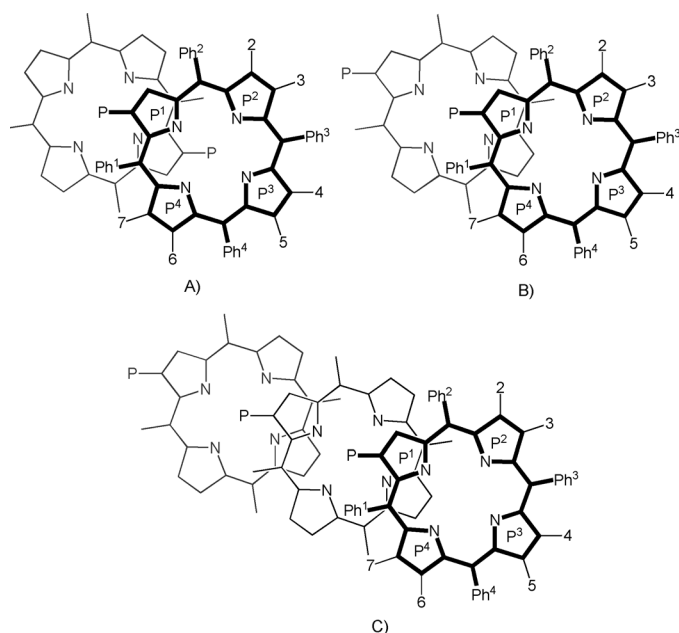


Figure 6. Schematic representation and designation of the protons of possible associated species of **1Zn** and **3Zn** in solution.

could be expected, that is, the formation of a dimer species through a single phosphoryl group coordination (Figure 6B) and a polymeric 1D-chain structure (Figure 6C).

It was shown, that temperature variations significantly influence the association process in both solvents. Although the spectrum of **1Zn** in  $\text{CDCl}_3$  at 303 K is significantly broadened, an increase of the temperature to 323 K results in a resolution gain through the suppression of the association. In this case all the resonances expected for the monomeric **1Zn** are observed and the spectrum becomes similar to the one observed in the  $\text{CDCl}_3/[\text{D}_4]\text{MeOH}$  solutions (see the Supporting Information, Table S1). The only exception is that the resonance pattern of the  $-\text{OCH}_2-$  diastereotopic protons differs from the one of **1Zn** in  $\text{CDCl}_3/[\text{D}_4]\text{MeOH}$ .

The temperature decrease to 223 K leads to the formation of more stable associates. The phosphorus signal is shifted upfield by  $\delta \approx 1$  ppm upon cooling of the sample (see the Supporting Information, Figure S9–S11). The observed change is in accordance with the formation of associated species of *meso*-mono-phosphorylated zinc porphyrins.<sup>[60,64]</sup> This small change of the chemical shift is the result of two opposite factors: the magnetic anisotropy of the  $\pi$  system of the porphyrin ring induces the upfield shift of the resonance peak. In contrast, the  $\text{P}=\text{O}\cdots\text{Zn}$  coordination leads to a downfield shift. This data allows to conclude, that the structure of associate A (Figure 6A) differs from that of dimer B (Figure 6B), because two phosphorus resonances are expected in the  $^{31}\text{P}\{^1\text{H}\}$  NMR spectrum for compound B.

A gradual temperature decrease of the **1Zn** solution from 323 to 223 K results in a significant evolution of the  $^1\text{H}$  NMR spectrum (Figure 7). Cooling the sample to 253 K leads to broadening and a shift of all the signals, whereas a further temperature decrease to 223 K affords a novel com-

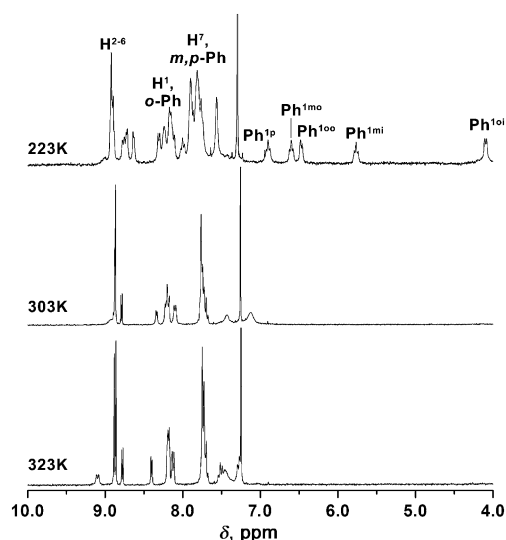


Figure 7. Variable-temperature  $^1\text{H}$  NMR spectra of **1Zn** in  $\text{CDCl}_3$  at 223 K (top), 303 K (middle), and 323 K (bottom).

licated set of resonances. This data are in accordance with a decreased symmetry of the possible associated species (Figure 6) compared to the starting Zn porphyrin.

A set of five multiplets in the  $\delta=4\text{--}7$  ppm range was attributed to the protons of the  $\text{Ph}^1$  substituent, which are non-equivalent and shielded by the adjacent porphyrin  $\pi$  system. The chemical shifts of the two doublets at  $\delta=4.09$  and  $6.47$  ppm of the *ortho* protons and the corresponding triplets at  $\delta=5.76$  and  $6.60$  ppm of the *meta* protons, are significantly different and correspond to all the associate forms given in Figure 6. The resonances of the inner-oriented *ortho* and *meta* protons occupy the most upfield position. Moreover, the obtained spectrum corresponds rather to dimer A than to oligomer C. Indeed, two sets of upfield-shifted resonances of five phenyl protons, namely  $\text{Ph}^1$  and  $\text{Ph}^3$ , are expected for oligomer C. The resonance pattern of the pyrrolic protons is also in agreement with structure A. Dimer A possesses only an inversion center, which is located in the middle of a Zn–Zn line. This determines a paired equivalence of the protons of two porphyrin molecules forming the dimer, but also results in the non-equivalence of all the protons within each particular porphyrin fragment. The multiplet at  $\delta\approx 8.9$  ppm corresponds to two pyrrole protons, whereas two doublets at  $\delta=8.72$  and  $8.63$  ppm correspond to one proton each. The pair of correlated signals of the pyrrole protons, each of them being overlapped with the resonances of the phenyl protons, are found at  $\delta=8.93$  and  $7.90$  ppm by correlation spectroscopy (COSY). These signals can be attributed to the  $\text{P}^{4(6)}$  and  $\text{P}^{4(7)}$  protons, respectively, because of their significant difference in the chemical shifts due to the influence of the  $\text{Ph}^1$  substituent discussed above. The doublet at  $\delta=8.31$  ppm can be assigned to the  $\text{P}^1$  proton, which is directly subjected to the shielding effect of the porphyrin  $\pi$  system in the dimeric species. Moreover, this signal is not correlated to any other signal.

We intended to finish the assignment of all the protons in dimer A by changing the solvent to the less polar  $[\text{D}_8]\text{toluene}$ , which should favor the **1Zn** association. Surprisingly, the obtained spectra were more complicated than the ones obtained in  $\text{CDCl}_3$ . One broad phosphorus signal is observed at 303 K (see the Supporting Information, Figure S13). At 323 K this signal was shifted downfield and became more narrow, proving that the aggregates were still present in solution (see the Supporting Information, Figure S14). The temperature decrease down to 223 K resulted not only in an upfield shift of the signal (see the Supporting Information, Figure S12), but also in its splitting into two components with a 1:1.4 intensity ratio showing that two diastereomers of dimer A could exist under these conditions. Although the  $(R_p, S_p)$  isomer is relevant to the X-ray data (Figure 1), the  $(+/-)-(R_p, R_p)$  isomer can be derived from the first one by the inversion of one of the porphyrin molecules (Figure 8). This diastereoisomer possesses only a  $C_2$  axis and exists as a pair of enantiomers, the phosphorus resonances of which must coincide.

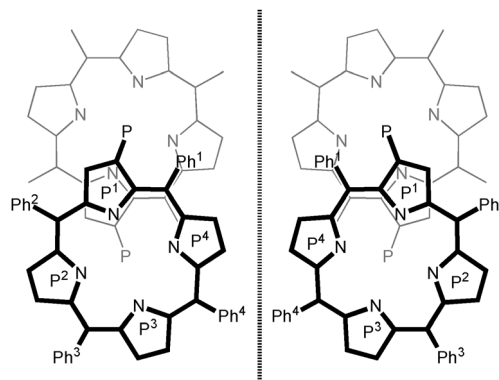


Figure 8. Enantiomeric pair of the presumed  $(+/-)-(R_p, R_p)$  diastereoisomer of dimer A.

The  $^1\text{H}$  NMR spectra of **1Zn** in  $[\text{D}_8]\text{toluene}$  are in agreement with this proposal (Figure 9). The spectrum at 303 K is broadened and an increase of the temperature to 323 K does not lead to a complete suppression of the dimerization. Nevertheless, the observed resonances can be partially assigned. Thus, three broad multiplets at  $\delta=8.10\text{--}8.35$ ,  $7.56\text{--}7.68$ , and  $7.53$  ppm correspond to the *ortho*, *meta*, and *para* protons of the *meso*-phenyl substituents, respectively (based on their chemical shifts and their integrals ratio of 2:2:1). Two narrow doublets at  $\delta=8.40$  and  $8.89$  ppm are coupled according to the COSY spectrum and can be assigned to the  $\beta$  protons of the  $\text{P}^4$  ring,  $\text{H}^7$  and  $\text{H}^6$ , respectively. Two broadened signals of the  $\text{P}^2$  and  $\text{P}^3$  protons are found in the  $\delta=8.96\text{--}9.04$  ppm range. A broad signal is observed at  $\delta\approx 8.63$  ppm and can be attributed to the  $\text{P}^1$  proton, because this proton is the most influenced by the partial dimerization.

The temperature decrease to 223 K slows down the exchange processes and a doubled set of narrow multiplets in

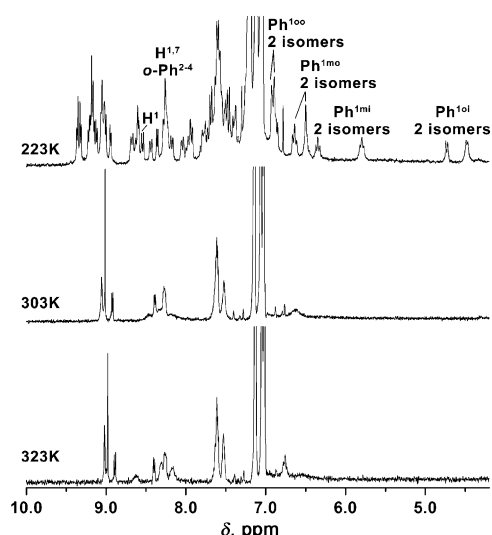


Figure 9.  $^1\text{H}$  NMR spectra of **1Zn** in  $[\text{D}_8]$ toluene at 223 (top), 303 (middle), and 323 K (bottom).

a 1:1.4 ratio is observed within the  $\delta = 4.0\text{--}10.0$  ppm spectral region of the spectrum (Figure 9). The assignment of the protons is not easy due to the overlap of the signals; however the assignment of the resonances in this region can be based on the relative intensities of signals and the COSY data. Close proximity of the observed subsets and equal number of observed resonances fit the symmetry of dimeric diastereoisomers A. The  $\delta = 4.4\text{--}7.0$  ppm spectral region is occupied by sub-sets of resonances, which are attributed to the protons of the  $\text{Ph}^1$  substituent, the most upfield signals are expected for inner-oriented *ortho* and *meta* protons. The set of doublets in the  $\delta = 9.40\text{--}8.30$  ppm region was attributed to the aromatic protons of the porphyrin core. The broad-band  $^{31}\text{P}$ -decoupling experiment allows for the assignment of the  $\text{P}^1$  protons. Six pairs of doublets corresponding to two subsets of the  $\text{P}^2$ ,  $\text{P}^3$ , and  $\text{P}^4$  protons are clearly identified by the COSY experiment. A slight difference of the chemical shifts ( $\delta \approx 0.05\text{--}0.1$  ppm) is observed within this series for four pairs of protons. In contrast, the other two pairs demonstrate the difference between the component resonances at  $\delta = 0.47$  and  $0.81$  ppm for the major and minor species, respectively. These pairs of signals are attributed to the protons of the  $\text{P}^4$  fragments as observed for the monomeric form of the compound at 323 K. The rotation barrier of the  $\text{Ph}^1$  substituent should be higher in the case of the dimer than for the monomeric form. Furthermore, its perpendicular orientation with respect to the porphyrin macrocycle is expected according to the presence of five distinct signals of this moiety in the upfield region. Consequently, the influence of magnetic anisotropy of this aromatic ring onto the  $\text{H}^7$  proton is presumed to be the same as in the monomeric form. Other pairs of resonances can be attributed to the  $\text{P}^2$  and  $\text{P}^3$  fragments of the two isomeric dimers. The precise assignment of all resonances of the  $\text{Ph}^2$ ,  $\text{Ph}^3$ , and  $\text{Ph}^4$  protons is not possible because of their signifi-

cant overlap. Nevertheless, twelve doublets are observed in the  $\delta = 9.1\text{--}7.6$  ppm region, which correlate with twelve triplet signals as revealed by the COSY experiment. These pairs can be attributed to the *ortho* and *meta* protons of six phenyl groups. The remaining protons of the phenyl groups are observed as a series of overlapped signals in the  $\delta = 7.2\text{--}7.8$  ppm region.

The spectral behavior of porphyrin **3Zn**, bearing isopropyl substituents at the phosphoryl groups, is similar to that of **1Zn**. Nevertheless, steric hindrance of the bulkier isopropyl substituents results in a less efficient association and less significant shifts of the resonances. Thus, a set of relatively narrow resonances is observed in the  $^1\text{H}$  NMR spectrum of **3Zn** in  $\text{CDCl}_3$  at 303 K, testifying that the derivative is predominantly in a monomeric form. The temperature increase to 323 K results in the spectrum relevant to the monomer **3Zn** (see the Supporting Information, Figures S6 and S7). The temperature decrease to 223 K results in a broadening of the signals without a notable shift of the resonances corresponding to a low degree of association. The association is enhanced in toluene (see the Supporting Information, Figure S8). The temperature decrease in  $[\text{D}_8]$ toluene shifts the monomer/dimer equilibrium and leads to the formation of two dimeric diastereomers A in a 1:1.7 ratio. The description of the  $^1\text{H}$  and  $^{31}\text{P}\{^1\text{H}\}$  NMR spectra is provided in the Supporting Information.

In conclusion, although a complete assignment of all the signals observed in the  $^1\text{H}$  NMR spectra of **1Zn** and **3Zn** at low temperatures was not possible due to the signals overlap, the obtained data allowed an unambiguous interpretation of the aggregate structure in solution. The behavior of **1Zn** and **3Zn** at different temperatures in different solvents is consistent with the self-aggregation leading to the formation of dimer A. Two diastereomers exist in solution and their ratio depends on the nature of the substituents and solvents.

## Conclusions

Metal-mediated carbon–phosphorous bond-forming reactions were successfully applied to the synthesis of  $\beta$ -(dialkoxyphosphoryl)porphyrins. An unusual one-pot sequence involving consecutive reduction and phosphorylation of  $\text{H}_2\text{TPPBr}_4$  provided bis(dialkoxy)phosphorylporphyrins in good yields.

According to X-ray studies, **1Zn** and **3Zn** exist as zinc  $\beta$ -phosphorylporphyrinate cofacial dimers formed by two  $\text{P}\cdots\text{O}\cdots\text{Zn}$  coordination bonds in the solid state. This self-organization is also observed in weakly polar solvents. The stability of these aggregates in solution is dependent on the nature of the alkoxy substituents of the dialkoxyphosphoryl group. Thus,  $\beta$ -phosphorylporphyrins can be viewed as new model compounds for a weakly coupled chlorophyll pair in photosynthesis and molecular precursors for the design of coordination polymers.

## Experimental Section

All chemicals used were of analytical grade and were purchased from Acros and Aldrich Co. unless stated otherwise. Silica gel (0.04–0.063 mm, 230–400 mesh ASTM, Merck) was used for column chromatography. Analytical thin-layer chromatography (TLC) was carried out by using Merck silica gel 60 plates (precoated sheets, 0.2 mm thick, with fluorescence indicator F254). [5,10,15,20-Tetraphenyl]porphyrin (H<sub>2</sub>TPP),<sup>[73]</sup> [2-bromo-5,10,15,20-tetraphenyl]porphyrin (H<sub>2</sub>TPPBr), and<sup>[60,64]</sup> [2,3,12,13-tetrabromo-5,10,15,20-tetraphenyl]porphyrin (H<sub>2</sub>TPPBr<sub>4</sub>)<sup>[62]</sup> were prepared and metallated<sup>[63]</sup> to afford [2-bromo-5,10,15,20-tetraphenylporphyrinato]zinc (ZnTPPBr) and [2,3,12,13-tetrabromo-5,10,15,20-tetraphenylporphyrinato]zinc (ZnTPPBr<sub>4</sub>) according to literature procedures.

**[2-(Diethoxyphosphoryl)-5,10,15,20-tetraphenylporphyrin (1H<sub>2</sub>):** A 15 mL round bottom flask equipped with a reflux condenser and a magnetic stir bar was charged with the bromoporphyrin H<sub>2</sub>TPPBr (25 mg, 0.036 mmol), Pd(OAc)<sub>2</sub> (8.1 mg, 0.036 mmol), and PPh<sub>3</sub> (28.3 mg, 0.108 mmol). The flask was then evacuated and purged with N<sub>2</sub> three times. Toluene (abs., 3 mL), diethylphosphite (55 μL, 0.432 mmol), and triethylamine (75 μL, 0.540 mmol) were added through a syringe and the resulting mixture was heated to reflux for 4 h until complete conversion of the bromide. Upon cooling the mixture was concentrated to give a solid, which was purified by column chromatography on silica gel by using CHCl<sub>3</sub> and hexane as eluent. The reddish-purple fraction (CHCl<sub>3</sub>/hexane, 80:20 (v/v)) was collected and concentrated to give **1H<sub>2</sub>** as a purple solid in 87% (23.5 mg) yield. <sup>1</sup>H NMR (600 MHz, CDCl<sub>3</sub>/CD<sub>3</sub>OD, 1:1 (v/v)): δ = 9.05 (d, *J* = 8.3 Hz, 1H; β-H), 8.51 (d, *J* = 4.4 Hz, 1H; β-H), 8.47 (d, *J* = 4.4 Hz, 1H; β-H), 8.39 (d, *J* = 4.4 Hz, 1H; β-H), 8.26 (m, 3H; β-H), 7.79 (m, 4H; *o*-Ph), 7.69 (m, 4H; *o*-Ph), 7.32 (m, 12H; *m*-Ph, *p*-Ph), 3.60 (m, 4H; CH<sub>2</sub>), 0.88 (t, *J* = 7.2 Hz, 6H; CH<sub>3</sub>), -3.00 ppm (s, 2H; NH); <sup>31</sup>P NMR (300 MHz, CDCl<sub>3</sub>/CD<sub>3</sub>OD, 1:1 (v/v)): δ = 16.5 ppm; MS (MALDI TOF): *m/z* calcd for (C<sub>48</sub>H<sub>39</sub>N<sub>4</sub>O<sub>3</sub>P)<sup>+</sup>: 750.3; found: 751 [M+H]<sup>+</sup>; IR (powder, micro-ATR):  $\tilde{\nu}$  = 1245 cm<sup>-1</sup> (P=O); UV/Vis (CHCl<sub>3</sub>): (log ε) λ<sub>max</sub> = 424 (5.34), 489 (sh), 522 (4.02), 559 (3.56), 599 (3.53), 656 nm (3.65).

**[2-(Diethoxyphosphoryl)-5,10,15,20-tetraphenylporphyrinato]zinc (1Zn):** The same procedure as for ZnTPPBr was applied and yielded the product in 78% (19.6 mg). <sup>1</sup>H NMR (600 MHz, CDCl<sub>3</sub>/CD<sub>3</sub>OD, 1:1 (v/v)): δ = 9.16 (d, *J* = 8.2 Hz, 1H; β-H), 8.48 (m, 2H; β-H), 8.45 (m, 2H; β-H), 8.36 (d, *J* = 4.5 Hz, 1H; β-H), 8.13 (d, *J* = 4.5 Hz, 1H; β-H), 7.83 (m, 8H; *o*-Ph), 7.40 (m, 12H; *m*-Ph, *p*-Ph), 3.66 (m, 4H; CH<sub>2</sub>), 0.95 ppm (t, *J* = 7.1 Hz, 6H; CH<sub>3</sub>); <sup>31</sup>P NMR (600 MHz, CDCl<sub>3</sub>/CD<sub>3</sub>OD, 1:1 (v/v)): δ = 18.2 ppm; MS (MALDI TOF): *m/z* calcd for (C<sub>48</sub>H<sub>39</sub>N<sub>4</sub>O<sub>3</sub>P)<sup>+</sup>: 752; found: 750.8 [M-Zn+H]<sup>+</sup>; MS (MALDI TOF): *m/z* calcd for (C<sub>48</sub>H<sub>37</sub>N<sub>4</sub>O<sub>3</sub>PZn)<sup>+</sup>: 812.2; found: 813 [M+H]<sup>+</sup>; IR (powder, micro-ATR):  $\tilde{\nu}$  = 1228 cm<sup>-1</sup> (P=O); UV/Vis (CHCl<sub>3</sub>): (log ε) λ<sub>max</sub> = 429 (5.49), 524 (sh), 562 (4.08), 604 nm (3.77).

**[2-(Dibutoxyphosphoryl)-5,10,15,20-tetraphenylporphyrinato]zinc (2Zn):** A 15 mL round bottom flask equipped with a reflux condenser and a magnetic stir bar was charged with the (bromoporphyrinato)zinc ZnTPPBr (20 mg, 0.026 mmol), CuI (15.1 mg, 0.079 mmol), and Cs<sub>2</sub>CO<sub>3</sub> (120.5 mg, 0.370 mmol). The flask was then evacuated and purged with N<sub>2</sub> three times. Toluene (abs., 3 mL), dibutylphosphite (124 μL, 0.634 mmol), and dimethylethylenediamine (60 μL, 0.555 mmol) were added through a syringe and the resulting mixture was heated to reflux for 12 h until complete conversion of the bromide. The mixture was then cooled and concentrated to give a solid, which was purified by column chromatography on silica gel by using CHCl<sub>3</sub> and hexane as eluent. The purple fraction (CHCl<sub>3</sub>/hexane, 60:40 (v/v)) was collected and evaporated to give **2Zn** as a purple solid in 94% (21.4 mg) yield. <sup>1</sup>H NMR (300 MHz, CDCl<sub>3</sub>/CD<sub>3</sub>OD, 1:1 (v/v)): δ = 9.16 (d, *J* = 8.1 Hz, 1H; β-H), 8.48 (m, 4H; β-H), 8.36 (d, *J* = 4.8 Hz, 1H; β-H), 8.13 (d, *J* = 4.8 Hz, 1H; β-H), 7.84 (m, 8H; *o*-Ph), 7.35 (m, 12H; *m*-Ph, *p*-Ph), 3.60 (m, 4H; CH<sub>2</sub>), 1.30 (m, 4H; CH<sub>2</sub>), 1.03 (m, 4H; CH<sub>2</sub>), 0.58 ppm (t, *J* = 7.4 Hz, 6H; CH<sub>3</sub>); <sup>31</sup>P NMR (300 MHz, CDCl<sub>3</sub>/CD<sub>3</sub>OD, 1:1 (v/v)): δ = 18.1 ppm; MS (MALDI TOF): *m/z* calcd for (C<sub>52</sub>H<sub>45</sub>N<sub>4</sub>O<sub>3</sub>PZn)<sup>+</sup>: 868.3; found: 870 [M+2H]<sup>+</sup>; IR (powder, micro-ATR):  $\tilde{\nu}$  = 1220 cm<sup>-1</sup> (P=O); UV/Vis (CHCl<sub>3</sub>): (log ε) λ<sub>max</sub> = 430 (5.60), 527 (sh), 562 (4.18), 605 nm (3.85).

**[2,12-(Diethoxyphosphoryl)-5,10,15,20-tetraphenylporphyrinato]zinc (5Zn) and [2,13-(diethoxyphosphoryl)-5,10,15,20-tetraphenylporphyrinato]zinc (6Zn):** A 15 mL round bottom flask equipped with a reflux condenser and a magnetic stir bar was charged with the bromoporphyrin H<sub>2</sub>TPPBr<sub>4</sub> (100 mg, 0.108 mmol), Pd(OAc)<sub>2</sub> (24.1 mg, 0.108 mmol), and PPh<sub>3</sub> (86.8 mg, 0.323 mmol). The flask was then evacuated and purged with N<sub>2</sub> three times. Toluene (abs., 9 mL), EtOH (abs., 6 mL), diethylphosphite (165 μL, 1.290 mmol), and triethylamine (225 μL, 1.613 mmol) were added through a syringe and the resulting mixture was heated to reflux for 5 days until complete conversion of the bromide. The mixture was then cooled and concentrated to give a solid, which was purified by column chromatography on silica gel by using CHCl<sub>3</sub> and hexane, followed by CHCl<sub>3</sub> and MeOH as eluent. The brown fraction (MeOH/CHCl<sub>3</sub>, 1:99 (v/v)) was collected and evaporated to give a mixture (1:1) of 2,12- and 2,13-diethoxyphosphoryl-5,10,15,20-tetraphenylporphyrins (**5H<sub>2</sub>** and **6H<sub>2</sub>**) (77.1 mg, 81%). The attempts to separate these porphyrins by using column chromatography were unsuccessful. The individual compounds were obtained as zinc complexes after metallation of the porphyrins mixture with Zn(OAc)<sub>2</sub>·2H<sub>2</sub>O by using the procedure described for ZnTPPBr. Purification by column chromatography on silica gel (MeOH/CHCl<sub>3</sub>, 1:99 (v/v)) allowed to isolate **5Zn** and **6Zn**.

**[2,12-(Diethoxyphosphoryl)-5,10,15,20-tetraphenylporphyrinato]zinc (5Zn):** <sup>1</sup>H NMR (600 MHz, CDCl<sub>3</sub>/CD<sub>3</sub>OD, 1:1 (v/v)): δ = 9.15 (d, *J* = 8.2 Hz, 2H; β-H), 8.39 (d, *J* = 4.7 Hz, 2H; β-H), 8.15 (d, *J* = 4.7 Hz, 2H; β-H), 7.84 (m, 4H; *o*-Ph), 7.81 (m, 4H; *o*-Ph), 7.42 (m, 8H; *m*-Ph), 7.30 (t, *J* = 7.7 Hz, 4H; *p*-Ph), 3.67 (m, 8H; CH<sub>2</sub>), 0.96 ppm (t, *J* = 7.1 Hz, 12H; CH<sub>3</sub>); <sup>31</sup>P NMR (600 MHz, CDCl<sub>3</sub>/CD<sub>3</sub>OD, 1:1 (v/v)): δ = 17.5 ppm; MS (MALDI TOF): *m/z* calcd for (C<sub>52</sub>H<sub>46</sub>N<sub>4</sub>O<sub>6</sub>P<sub>2</sub>Zn)<sup>+</sup>: 950.3; found: 950 [M]<sup>+</sup>; IR (powder, micro-ATR):  $\tilde{\nu}$  = 1232 cm<sup>-1</sup> (P=O); UV/Vis (CHCl<sub>3</sub>): (log ε) λ<sub>max</sub> = 431 (5.03), 504 (sh), 525 (sh), 566 (3.62), 612 nm (3.58).

**[2,13-(Diethoxyphosphoryl)-5,10,15,20-tetraphenylporphyrinato]zinc (6Zn):** <sup>1</sup>H NMR (600 MHz, CDCl<sub>3</sub>/CD<sub>3</sub>OD, 1:1 (v/v)): δ = 9.10 (d, *J* = 8.2 Hz, 2H; β-H), 8.46 (s, 2H; β-H), 7.96 (s, 2H; β-H), 7.82 (dd, *J* = 7.7, 1.6 Hz, 4H; *o*-Ph), 7.74 (d, *J* = 7.7 Hz, 4H; *o*-Ph), 7.33 (m, 12H; *m*-Ph, *p*-Ph), 3.62 (m, 8H; CH<sub>2</sub>), 0.92 ppm (t, *J* = 7.1 Hz, 12H; CH<sub>3</sub>); <sup>31</sup>P NMR (600 MHz, CDCl<sub>3</sub>/CD<sub>3</sub>OD, 1:1 (v/v)): δ = 17.5 ppm; MS (MALDI TOF): *m/z* calcd for (C<sub>52</sub>H<sub>46</sub>N<sub>4</sub>O<sub>6</sub>P<sub>2</sub>Zn)<sup>+</sup>: 950.3; found: 950 [M]<sup>+</sup>; IR (powder, micro-ATR):  $\tilde{\nu}$  = 1240 cm<sup>-1</sup> (P=O); UV/Vis (CHCl<sub>3</sub>): (log ε) λ<sub>max</sub> = 433 (4.85), 500 (sh), 529 (sh), 566 (3.44), 612 nm (3.36).

**[2-(Diisopropoxyphosphoryl)-5,10,15,20-tetraphenylporphyrinato]zinc (3Zn):** A 15 mL round bottom flask equipped with a reflux condenser and a magnetic stir bar was charged with the (bromoporphyrinato)zinc ZnTPPBr (20 mg, 0.026 mmol), CuI (15 mg, 0.079 mmol), and Cs<sub>2</sub>CO<sub>3</sub> (121 mg, 0.370 mmol). The flask was then evacuated and purged with N<sub>2</sub> three times. Toluene (abs., 3 mL), diisopropylphosphite (106 μL, 0.634 mmol), and dimethylethylenediamine (60 μL, 0.555 mmol) were added through a syringe and the resulting mixture was heated to reflux for 2 days until complete conversion of the bromide. The mixture was then cooled and concentrated to give a solid, which was purified by column chromatography on silica gel by using CH<sub>2</sub>Cl<sub>2</sub> and methanol as eluent. The purple fraction (CH<sub>2</sub>Cl<sub>2</sub>/methanol, 99:1 (v/v)) was collected and evaporated to give **3Zn** as a purple solid in 86% (18.9 mg) yield. <sup>1</sup>H NMR (300 MHz, CDCl<sub>3</sub>/CD<sub>3</sub>OD, 3:2 (v/v)): δ = 9.24 (d, *J* = 8.4 Hz, 1H; β-H), 8.59 (m, 2H; β-H), 8.55 (m, 2H; β-H), 8.45 (d, *J* = 4.8 Hz, 1H; β-H), 8.20 (d, *J* = 4.8 Hz, 1H; β-H), 7.92 (m, 8H; *o*-Ph), 7.43 (m, 12H; *m*-Ph, *p*-Ph), 4.36 (m, 2H; CH), 1.02 (m, 6H; *J* = 6.2 Hz, CH<sub>3</sub>), 0.98 ppm (m, 6H; *J* = 6.2 Hz, CH<sub>3</sub>); <sup>31</sup>P NMR (300 MHz, CDCl<sub>3</sub>/CD<sub>3</sub>OD, 3:2 (v/v)): δ = 14.9 ppm; HRMS (ESI, positive mode): *m/z* calcd for (C<sub>50</sub>H<sub>41</sub>N<sub>4</sub>NaO<sub>3</sub>PZn)<sup>+</sup>: 863.21000; found: 863.20792 [M+Na]<sup>+</sup>; IR (powder, micro-ATR):  $\tilde{\nu}$  = 1230 (sh), 1213 cm<sup>-1</sup> (P=O); UV/Vis (CHCl<sub>3</sub>): (log ε) λ<sub>max</sub> = 431 (5.56), 565 (4.18), 607 nm (3.93).

**[2-(Dibutoxyphosphoryl)-5,10,15,20-tetraphenylporphyrin (2H<sub>2</sub>):** A 15 mL round bottom flask equipped with a reflux condenser and a magnetic stir bar was charged with the bromoporphyrin H<sub>2</sub>TPPBr (18.5 mg, 0.026 mmol), Pd(OAc)<sub>2</sub> (6 mg, 0.026 mmol), and PPh<sub>3</sub> (21 mg, 0.08 mmol). The flask was then evacuated and purged with N<sub>2</sub> three times. Toluene (abs., 3 mL), dibutylphosphite (62 μL, 0.32 mmol), and

triethylamine (56  $\mu$ L, 0.4 mmol) were added through a syringe and the resulting mixture was heated to reflux for 2 days until complete conversion of the bromide. After cooling the mixture was concentrated to give a solid, which was purified by column chromatography on silica gel by using  $\text{CH}_2\text{Cl}_2$  and methanol as eluent. The reddish-purple fraction ( $\text{CH}_2\text{Cl}_2$ /methanol, 99.5:0.5 (v/v)) was collected and concentrated to give **2H<sub>2</sub>** as a purple solid in 92% (19.8 mg) yield.  $^1\text{H}$  NMR (300 MHz,  $\text{CDCl}_3/\text{CD}_3\text{OD}$ , 3:2 (v/v)):  $\delta$  = 9.12 (d,  $J$  = 8.2 Hz, 1H;  $\beta$ -H), 8.65 (m, 2H;  $\beta$ -H), 8.53 (d,  $J$  = 5.0 Hz, 1H;  $\beta$ -H), 8.48 (m, 2H;  $\beta$ -H), 8.34 (d,  $J$  = 5.0 Hz, 1H;  $\beta$ -H), 7.94 (m, 8H; *o*-Ph), 7.48 (m, 12H; *m*-Ph, *p*-Ph), 3.63 (m, 4H;  $\text{CH}_2$ ), 1.34 (m, 4H;  $\text{CH}_2$ ), 1.08 (m, 4H;  $\text{CH}_2$ ), 0.63 ppm (t,  $J$  = 7.3 Hz, 6H;  $\text{CH}_3$ );  $^{31}\text{P}$  NMR (300 MHz,  $\text{CDCl}_3/\text{CD}_3\text{OD}$ , 3:2 (v/v)):  $\delta$  = 16.2 ppm; HRMS (ESI, positive mode):  $m/z$  calcd for  $(\text{C}_{52}\text{H}_{47}\text{N}_4\text{NaO}_3\text{P})^+$ : 829.32835; found: 829.32813  $[\text{M}+\text{Na}]^+$ ; HRMS (ESI, positive mode):  $m/z$  calcd for  $(\text{C}_{104}\text{H}_{94}\text{N}_8\text{NaO}_3\text{P})^+$ : 1636.67028; found: 1636.66901  $[\text{2M}+\text{Na}]^+$ ; IR (powder, micro-ATR):  $\tilde{\nu}$  = 1250 (P=O), 3330  $\text{cm}^{-1}$  (NH); UV/Vis ( $\text{CHCl}_3$ ): ( $\log \epsilon$ )  $\lambda_{\text{max}}$  = 424 (5.59), 523 (4.26), 558 (3.76), 599 (3.69), 656 nm (3.81).

**Spectroscopic measurements:**  $^1\text{H}$ ,  $^{13}\text{C}$ , and  $^{31}\text{P}$  NMR spectra were recorded on a Bruker Avance II 300 and a Bruker Avance III 600. All chemical shifts are given in [ppm], referenced on the  $\delta$  scale by using the residual solvent peak as internal standard for  $^1\text{H}$  and  $^{13}\text{C}$  NMR spectroscopy, and phosphoric acid ( $\text{H}_3\text{PO}_4$ ) for  $^{31}\text{P}$  NMR spectroscopy. UV/Vis spectra were recorded with a Varian Cary 100 spectrophotometer. Mass spectra were obtained in linear mode with a Bruker Proflex III MALDI-TOF mass spectrometer by using dithranol as matrix and accurate mass measurements (HRMS) by using a Bruker microTOF-Q ESI-TOF mass spectrometer. IR spectra were registered on a FTIR Nexus (Nicolet) spectrophotometer. Micro-ATR accessory (Pike) was used in order to obtain IR spectra of polycrystalline solid complexes.

**X-ray crystallographic analysis:** Single-crystal X-ray diffraction experiments for complexes of **1Zn** and **3Zn** were carried out on a Bruker SMART APEX II diffractometer with a CCD area detector (graphite monochromator,  $\text{MoK}_\alpha$  radiation,  $\lambda$  = 0.71073 Å,  $\omega$  scans). The single crystals of **1Zn** were slightly reflected in  $\theta > 22^\circ$ . The attempts to grow single crystals by slow evaporation from methanol/benzene/ $\text{CHCl}_3$  or methanol/benzene/heptane at room temperature or  $5^\circ\text{C}$  were unsuccessful; slow diffusion of heptanes into methanol/benzene or methanol/benzene/ $\text{CHCl}_3$  also did not lead to the formation of single crystals. The OEt fragment (O(2), C(45), C(46)) in **1Zn** are disordered. There are disordered molecules of methanol and water with a multiplicity 0.5 in the crystal packing cell of **3Zn**. The semi-empirical method SADABS was applied for the absorption correction.<sup>[74]</sup> The structures were solved by direct methods and refined by the full-matrix least-squares technique against  $F^2$  with the anisotropic displacement parameters for all non-hydrogen atoms. All the hydrogen atoms were placed geometrically and included in the structure factors calculation in the riding motion approximation. All the data reduction and further calculations were performed by using the SAINT and SHELXTL-97 program packages.<sup>[75,76]</sup> CCDC-842626 (**1Zn**) and CCDC-842627 (**3Zn**) contain the supplementary crystallographic data for this paper. These data can be obtained free of charge from The Cambridge Crystallographic Data Centre via [www.ccdc.cam.ac.uk/data\\_request/cif](http://www.ccdc.cam.ac.uk/data_request/cif).

**X-ray crystal structure data for (1Zn)<sub>2</sub>·2C<sub>6</sub>H<sub>6</sub>:** Formula:  $\text{C}_{108}\text{H}_{86}\text{N}_8\text{O}_6\text{P}_2\text{Zn}_2$ ; monoclinic; crystal size:  $0.06 \times 0.03 \times 0.02$  mm; space group  $C2/c$ ;  $a$  = 36.91(3),  $b$  = 11.194(10),  $c$  = 24.70(2) Å;  $\alpha$  = 90,  $\beta$  = 122.78(2),  $\gamma$  = 90°;  $V$  = 8578(14) Å<sup>3</sup>;  $Z$  = 8(4),  $D_{\text{calcd}}$  = 1.382  $\text{Mg m}^{-3}$ ;  $2q_{\text{max}}$  = 136.48;  $T$  = 173(2) K;  $\mu$  = 1.084  $\text{mm}^{-1}$ ;  $T_{\text{min}}$  = 0.947;  $T_{\text{max}}$  = 0.736; 35256 measured reflections; 16846 independent reflections ( $R_{\text{int}}$  = 0.1566); 7463 refined parameters;  $R$  = 0.0917;  $wR_2$  = 0.1524.

**X-ray crystal structure data for (3Zn)<sub>2</sub>·H<sub>2</sub>O·CH<sub>3</sub>COOH:** Formula:  $\text{C}_{104}\text{H}_{100}\text{N}_8\text{O}_{12}\text{P}_2\text{Zn}_2$ ; triclinic; crystal size:  $0.14 \times 0.12 \times 0.10$  mm; space group  $P\bar{1}$ ;  $a$  = 11.552(2),  $b$  = 13.355(3),  $c$  = 16.383(3) Å;  $\alpha$  = 83.292(3),  $\beta$  = 72.131(3),  $\gamma$  = 79.394(3)°;  $V$  = 2359.6(8) Å<sup>3</sup>;  $Z$  = 2(1);  $D_{\text{calcd}}$  = 1.288  $\text{Mg m}^{-3}$ ;  $2q_{\text{max}}$  = 136.48;  $T$  = 173(2) K;  $\mu$  = 1.084  $\text{mm}^{-1}$ ;  $T_{\text{min}}$  = 0.947;  $T_{\text{max}}$  = 0.736; 35256 measured reflections; 19300 independent reflections ( $R_{\text{int}}$  = 0.0859); 8273 refined parameters;  $R1$  = 0.0717;  $wR_2$  = 0.1647.

## Acknowledgements

This work was supported by the CNRS, the ARCUS Burgundy-Russia project (2007–2010), the Russian Foundation for Basic Research (grant no. 12-03-93110), and was carried out in the frame of the International Associated French–Russian Laboratory of Macrocyclic Systems and Related Materials (LAMREM) of CNRS. The authors thank Dr. A. N. Molokanov for helpful discussions concerning this work.

- [1] K. M. Kadish, K. M. Smith, R. Guilard in *The Porphyrin Handbook*, World Scientific, Singapore, **2010**.
- [2] T. Patrice in *Photodynamic Therapy*, RSC, London, **2004**.
- [3] A. E. O'Connor, W. M. Gallagher, A. T. Byrne, *Photochem. Photobiol.* **2009**, *85*, 1053–1074.
- [4] M. Ethirajan, Y. Chen, P. Joshi, R. K. Pandey, *Chem. Soc. Rev.* **2011**, *40*, 340–362.
- [5] E. J. Kim, H. R. Yang, S. J. Lee, G. Y. Kim, C. H. Kwak, *Opt. Express* **2008**, *16*, 17329–17341.
- [6] M. Tian, J. Zhang, I. Lorgeté, J. P. Galaup, J. L. Le Gouët, *J. Opt. Soc. Am. B* **1998**, *15*, 2216–2225.
- [7] R. T. Kuznetsova, T. N. Kopylova, G. V. Mayer, L. G. Samsonova, V. A. Svetlichnyi, A. V. Vasil'ev, D. N. Filinov, E. N. Tel'minov, N. S. Kabotaeva, N. V. Svarovskaya, V. M. Podgaetskii, A. V. Reznichenko, *Quantum Electron.* **2004**, *34*, 139–146.
- [8] D. Dini, G. Y. Yang, M. Hanack, *Targets Heterocycl. Syst.* **2004**, *8*, 1–32.
- [9] W.-K. Wong, X. Zhu, W.-Y. Wong, *Coord. Chem. Rev.* **2007**, *251*, 2386–2399.
- [10] S. Fu, X. Zhu, G. Zhou, W.-Y. Wong, C. Ye, W.-K. Wong, Z. Li, *Eur. J. Inorg. Chem.* **2007**, 2004–2013.
- [11] Z. B. Liu, J. G. Tian, Z. Guo, D. M. Ren, F. Du, J. Y. Zheng, Y. S. Chen, *Adv. Mater.* **2008**, *20*, 511–515.
- [12] M. Biesaga, K. Pyrzynska, M. Trojanowicz, *Talanta* **2000**, *51*, 209–224.
- [13] P. D. Beer, D. P. Cormode, J. J. Davis, *Chem. Commun.* **2004**, 414–415.
- [14] Y. Zhang, W. Xiang, R. Yang, F. Liu, K. Li, *J. Photochem. Photobiol. A* **2005**, *173*, 264–270.
- [15] A. Shundo, J. Labuta, J. P. Hill, S. Ishihara, K. Ariga, *J. Am. Chem. Soc.* **2009**, *131*, 9494–9495.
- [16] M. R. Wasielewski, *Chem. Rev.* **1992**, *92*, 435–461.
- [17] J.-C. Chambron, V. Heitz, J.-P. Sauvage in *The Porphyrin Handbook*, Vol. 6 (Eds.: K. M. Kadish, K. M. Smith, R. Guilard), Academic Press, San Diego, **2000**, pp. 1–42.
- [18] I. Beletskaya, V. S. Tyurin, A. Y. Tsvadze, R. Guilard, C. Stern, *Chem. Rev.* **2009**, *109*, 1659–1713.
- [19] P. D. Harvey, C. Stern, R. Guilard in *Handbook of Porphyrin Science*, Vol. 11 (Eds.: K. M. Kadish, K. M. Smith, R. Guilard), World Scientific Publishing, Singapore, **2011**, pp. 1–180.
- [20] J.-H. Chou, M. E. Kosal, H. S. Nalwa, N. A. Rakow, K. S. Suslick in *The Porphyrin Handbook*, Vol. 6 (Eds.: K. M. Kadish, K. M. Smith, R. Guilard), Academic Press, San Diego, **2000**, pp. 43–131.
- [21] Y. Matano, K. Matsumoto, Y. Terasaka, H. Hotta, Y. Araki, O. Ito, M. Shiro, T. Sasamori, N. Tokitoh, H. Imahori, *Chem. Eur. J.* **2007**, *13*, 891–901.
- [22] Y. Matano, K. Matsumoto, Y. Nakao, H. Uno, S. Sakaki, H. Imahori, *J. Am. Chem. Soc.* **2008**, *130*, 4588–4589.
- [23] F. Atefi, J. C. McMurtrie, P. Turner, M. Duriska, D. P. Arnold, *Inorg. Chem.* **2006**, *45*, 6479–6489.
- [24] F. Atefi, J. C. McMurtrie, D. P. Arnold, *Dalton Trans.* **2007**, 2163–2170.
- [25] F. Atefi, D. P. Arnold, *J. Porphyrins Phthalocyanines* **2008**, *12*, 801–831.
- [26] Y. Y. Enakieva, A. G. Bessmertnykh, Y. G. Gorbunova, C. Stern, Y. Roussel, A. Y. Tsvadze, R. Guilard, *Org. Lett.* **2009**, *11*, 3842–3845.

- [27] K. M. Kadish, P. Chen, Y. Y. Enakieva, S. E. Nefedov, Y. G. Gorbunova, A. Y. Tsivadze, A. Bessmertnykh-Lemeune, C. Stern, R. Guillard, *J. Electroanal. Chem.* **2011**, *656*, 61–71.
- [28] W. M. Sharman, J. E. Van Lier, *J. Porphyrins Phthalocyanines* **2000**, *4*, 441–453.
- [29] J.-i. Setsune, *J. Porphyrins Phthalocyanines* **2004**, *8*, 93–102.
- [30] C. Liu, Q.-Y. Chen, *Synlett* **2005**, 1306–1310.
- [31] T. Takanami, M. Hayashi, H. Chijimatsu, W. Inoue, K. Suda, *Org. Lett.* **2005**, *7*, 3937–3940.
- [32] G. Bringmann, S. Rüdenauer, D. C. G. Götz, T. A. M. Gulder, M. Reichert, *Org. Lett.* **2006**, *8*, 4743–4746.
- [33] L. J. Esdaile, M. O. Senge, D. P. Arnold, *Chem. Commun.* **2006**, 4192–4194.
- [34] J.-P. Tremblay-Morin, H. Ali, J. E. van Lier, *Tetrahedron Lett.* **2006**, *47*, 3043–3046.
- [35] C. Liu, D.-M. Shen, Q.-Y. Chen, *J. Org. Chem.* **2007**, *72*, 2732–2736.
- [36] M. Beyler, C. Beemelmanns, V. Heitz, J.-P. Sauvage, *Eur. J. Org. Chem.* **2009**, 2801–2805.
- [37] M. A. Filatov, R. Guillard, P. D. Harvey, *Org. Lett.* **2010**, *12*, 196–199.
- [38] J. Song, N. Aratani, P. Kim, D. Kim, H. Shinokubo, A. Osuka, *Angew. Chem.* **2010**, *122*, 3699–3702; *Angew. Chem. Int. Ed.* **2010**, *49*, 3617–3620.
- [39] K. M. Smith, K. C. Langry, *J. Org. Chem.* **1983**, *48*, 500–506.
- [40] O. M. Minnetian, I. K. Morris, K. M. Snow, K. M. Smith, *J. Org. Chem.* **1989**, *54*, 5567–5574.
- [41] D. P. Arnold, L. J. Nitschinsk, *Tetrahedron Lett.* **1993**, *34*, 693–696.
- [42] S. G. DiMugno, V. S. Y. Lin, M. J. Therien, *J. Am. Chem. Soc.* **1993**, *115*, 2513–2515.
- [43] S. G. DiMugno, V. S. Y. Lin, M. J. Therien, *J. Org. Chem.* **1993**, *58*, 5983–5993.
- [44] H. Ali, J. E. van Lier, *Tetrahedron* **1994**, *50*, 11933–11944.
- [45] K. S. Chan, X. Zhou, B.-s. Luo, T. C. W. Mak, *J. Chem. Soc. Chem. Commun.* **1994**, 271–272.
- [46] X. Zhou, Z.-y. Zhou, T. C. W. Mak, K. S. Chan, *J. Chem. Soc. Perkin Trans. 1* **1994**, 2519–2520.
- [47] R. Bonnett, I. H. Campion-Smith, A. N. Kozyrev, A. F. Mironov, *J. Chem. Res. Synop.* **1990**, 138–139.
- [48] D. Mandon, P. Ochenbein, J. Fischer, R. Weiss, K. Jayaraj, R. N. Austin, A. Gold, P. S. White, O. Brügaud, *Inorg. Chem.* **1992**, *31*, 2044–2049.
- [49] M. G. H. Vicente in *The Porphyrin Handbook, Vol. 1* (Eds.: K. M. Kadish, K. M. Smith, R. Guillard), Academic Press, San Diego, **2000**, pp. 149–199.
- [50] L.-M. Jin, L. Chen, J.-J. Yin, J.-M. Zhou, C.-C. Guo, Q.-Y. Chen, *J. Org. Chem.* **2006**, *71*, 527–536.
- [51] L. Jaquinod in *The Porphyrin Handbook, Vol. 1* (Eds.: K. M. Kadish, K. M. Smith, R. Guillard), Academic Press, San Diego, **2000**, pp. 201–223.
- [52] D. E. Chumakov, A. V. Khoroshutin, A. V. Anisimov, K. I. Kobrakov, *Chem. Heterocycl. Compd.* **2009**, *45*, 259–283.
- [53] T. G. Traylor, S. Tsuchiya, *Inorg. Chem.* **1987**, *26*, 1338–1339.
- [54] P. Hoffmann, G. Labat, A. Robert, B. Meunier, *Tetrahedron Lett.* **1990**, *31*, 1991–1994.
- [55] P. Bhyrappa, V. Krishnan, *Inorg. Chem.* **1991**, *30*, 239–245.
- [56] P. Hoffmann, A. Robert, B. Meunier, *Bull. Soc. Chim. Fr.* **1992**, *129*, 85–97.
- [57] M. S. Chorghade, D. Dolphin, D. Dupré, D. R. Hill, E. C. Lee, T. P. Wijesekera, *Synthesis* **1996**, 1320–1324.
- [58] G. A. Spyroulias, A. P. Despotopoulos, C. P. Raptopoulou, A. Terzis, D. de Montauzon, R. Poilblanc, A. G. Coutsolelos, *Inorg. Chem.* **2002**, *41*, 2648–2659.
- [59] D.-M. Shen, C. Liu, Q.-Y. Chen, *Chem. Commun.* **2005**, 4982–4984.
- [60] G.-Y. Gao, J. V. Ruppel, D. B. Allen, Y. Chen, X. P. Zhang, *J. Org. Chem.* **2007**, *72*, 9060–9066.
- [61] L. Jaquinod, R. G. Khoury, K. M. Shea, K. M. Smith, *Tetrahedron* **1999**, *55*, 13151–13158.
- [62] K.-L. Li, C.-C. Guo, Q.-Y. Chen, *Synlett* **2009**, 2867–2871.
- [63] P. K. Kumar, P. Bhyrappa, B. Varghese, *Tetrahedron Lett.* **2003**, *44*, 4849–4851.
- [64] H. J. Callot, *Tetrahedron Lett.* **1973**, *14*, 4987–4990.
- [65] D. Gelman, L. Jiang, S. L. Buchwald, *Org. Lett.* **2003**, *5*, 2315–2318.
- [66] M. Kalek, J. Stawinski, *Organometallics* **2008**, *27*, 5876–5888.
- [67] For an example of a Stille reaction, see: T. Chandra, B. J. Kraft, J. C. Huffman, J. M. Zaleski, *Inorg. Chem.* **2003**, *42*, 5158–5172. For an example of a Suzuki reaction, see: P. Bhyrappa, M. Sankar, B. Varghese, *Inorg. Chem.* **2006**, *45*, 4136–4149.
- [68] T. Hirao, T. Masunaga, Y. Ohshiro, T. Agawa, *J. Org. Chem.* **1981**, *46*, 3745–3747.
- [69] S. Abbas, C. J. Hayes, S. Worden, *Tetrahedron Lett.* **2000**, *41*, 3215–3219.
- [70] G. Evano, K. Tadiparthi, F. Couty, *Chem. Commun.* **2011**, *47*, 179–181.
- [71] J. Deisenhofer, O. Epp, I. Sinning, H. Michel, *J. Mol. Biol.* **1995**, *246*, 429–457.
- [72] P. Jordan, P. Fromme, H. T. Witt, O. Klukas, W. Saenger, N. Krauss, *Nature* **2001**, *411*, 909–917.
- [73] A. D. Adler, F. R. Longo, J. D. Finarelli, J. Goldmacher, J. Assour, L. Korsakoff, *J. Org. Chem.* **1967**, *32*, 476.
- [74] SADABS, G. M. Sheldrick, Bruker AXS Inc., Madison, **1997**.
- [75] SHELXTL-97 V5.10, G. M. Sheldrick, Bruker AXS Inc., **1997**.
- [76] SMART V5.051 and SAINT V5.00, area detector control and integration software, Bruker AXS Inc., **1998**.

Received: July 23, 2012  
Published online: October 5, 2012